รายงานวิจัยฉบับสมบูรณ์

โครงการ การศึกษาการบาดเจ็บของไมโครวิลไลบนผิวของเซลล์ท่อไตส่วนปลายที่ถูกเกาะจับโดยผลึกแคลเซี่ยมอ๊อกซาเลท

โดย ดร.เกศรินทร์ ฟองเงิน

25 พฤษภาคม 2558

สัญญาเลขที่ TRG5680008

รายงานวิจัยฉบับสมบูรณ์

โครงการ การศึกษาการบาดเจ็บของไมโครวิลไลบนผิวของเซลล์ท่อไตส่วนปลายที่ถูกเกาะจับโดยผลึกแคลเซี่ยมอ๊อกซาเลท

ผู้วิจัย ดร.เกศรินทร์ ฟองเงิน
หน่วยโปรตีโอมิกส์ทางการแพทย์ สถานส่งเสริมการวิจัย
คณะแพทยศาสตร์ศิริราชพยาบาล มหาวิทยาลัยมหิดล

สนับสนุนโดยสำนักงานกองทุนสนับสนุนการวิจัย
และมหาวิทยาลัยมหิดล

Acknowledgement

This study was supported by The Thailand Research Fund (TRG5680008) and Mahidol University. The achievement of this project was assisted by the full supervision from Prof. Visith Thongboonkerd. I am extremely grateful for his assistance, valuable guidance and suggestions throughout this research project. I wish to thank the members of Medical Proteomics Unit for their consistent support, encouragement and kindness during this project.

Finally, I am absolutely thankful to TRF and Faculty of Medicine Siriraj Hospital, Mahidol University for all financial supports and appreciated prospect to perform this project.

Dr. Kedsarin Fong-ngern

Abstract

Project Code: TRG5680008

Project Title: Investigations of microvillar injury in renal tubular epithelial cells induced by calcium oxalate crystal adhesion

Investigator: Kedsarin Fong-ngern, Ph.D., Medical Proteomics Unit, Office for Research and Development, Faculty of Medicine Siriraj Hospital, Mahidol University, Bangkok, Thailand

E-mail Address: kedkai010@hotmail.com

Project Period: 2 years

The binding of calcium oxalate monohydrate (COM) crystal frequently results in the destruction of microvilli leading to renal tubular epithelial cell injury and dysfunction in stone patients. This study focused on the investigation of molecular mechanisms implicating in microvillar injuries and disorganization during COM crystal treatment in MDCK cells. Morphology of COM crystal-treated cells (48 h of incubation) was seriously changed as well as microvilli density covering their apical surface was also decreased. We found the reduction of ezrin which plays role in microvilli formation and stabilization in whole cell lysate extracted from COM crystal-treated cells by Western blot analysis. The localization of the remaining ezrin was also changed and concentrated at the lateral boundary of in COM crystal-treated cells under laser scanning confocal microscope. Selectively decreases of ezrin and actin cytoskeleton at the apical membrane were observed together with the loss of their association upon COM crystal exposure by performing Triton X-100 solubility assay. The use of antioxidant chemical, epigallocatechin-3-gallate (EGCG) pretreatment could reduce the degree of protein oxidation and also prevented the reduction and stabilize apical localization of ezrin and actin cytoskeleton after COM crystal treatment under confocal microscope. These findings may provide some important information as a platform to understand the pathogenesis leading to the loss of microvillar functions for a potential therapeutic benefit for kidney stone disease.

Keywords: Kidney stone disease, Calcium oxalate, Microvillar injury, Renal tubular cell dysfunction

บทคัดย่อ

รหัสโครงการ: TRG5680008

ชื่อโครงการ:การศึกษาการบาดเจ็บของไมโครวิลไลบนผิวของเซลล์ท่อไตส่วนปลายที่ถูกเกาะจับโดยผลึกแคลเซี่ยมอ๊อกซาเลท

ชื่อนักวิจัย: ดร.เกศรินทร์ ฟองเงิน สังกัดหน่วยโปรตีโอมิกส์ทางการแพทย์ สถานส่งเสริมการวิจัย คณะแพทยศาสตร์ศิริราชพยาบาล มหาวิทยาลัยมหิดล

E-mail Address: kedkai010@hotmail.com

ระยะเวลาโครงการ : 2 ปี

การเกาะจับของผลึกแคลเซี่ยมอ๊อกซาเลทชนิดโมโนไฮเดรตบนไมโครวิลไลของเซลล์ท่อไตมักเป็นสาเหตุก่อให้เกิดโรคนิ่วในไต อีกทั้งยังนำไปสู่การบาดเจ็บและการสูญเสียการทำหน้าที่ของเซลล์ท่อไตที่พบในผู้ป่ายโรคนิ่ว การศึกษาวิจัยนี้ได้มุ่งเป้าไปยังการสืบค้นหากลไกที่เกี่ยวข้องในการเกิดการบาดเจ็บและการเกิดพยาธิสภาพของไมโครวิลไลบนผิวของเซลล์ท่อไตส่วนปลาย Madin-Darby Canine Kidney (MDCK) เซลล์ จากการศึกษาวิจัยพบว่าลักษณะและความหนาแน่นของไมโครวิลไลบนผิวของเซลล์ท่อไตหลังจากที่ถูกเกาะจับโดยผลึกแคลเซี่ยมอ๊อกซาเลทเป็นเวลา 48 ชั่วโมงนั้น มีการเปลี่ยนแปลงและลดลงอย่างเห็นได้ชัด นอกจากนี้ยังพบว่าระดับการแสดงออกของโปรตีน ezrin ซึ่งเป็นโปรตีนหลักที่ทำหน้าที่สำคัญในการสร้างและรักษาสภาพของไมโครวิลไลนั้นลดลงและมีการเปลี่ยนแปลงย้ายตำแหน่งที่อยู่ในเซลล์ท่อไตหลังจากที่ถูกเกาะจับโดยผลึกแคลเซี่ยมอ๊อกซาเลท ทั้งนี้ยังพบว่าโปรตีน ezrin และ F-actin ซึ่งเป็นองค์ประกอบหลักของไมโครวิลไลได้ลดลงเฉพาะบริเวณที่ผิวเซลล์เท่านั้น นอกจากนี้ได้มีการใช้สารต้านอนุมูลอิสระที่สกัดมาจากชาเขียว epigallocatechin-3-gallate (EGCG) และพบว่าสามารถลดระดับการเกิดออกซิเดชั่นของโปรตีนพร้อมทั้งสามารถป้องกันการลดระดับลงของโปรตีน ezrin รวมไปถึงสามารถป้องกันการลดลงของโปรตีน ezrin และ F-actin ที่ตำแหน่งผิวเซลล์ท่อไตหลังจากที่ถูกเกาะจับโดยผลึกแคลเซี่ยมอ๊อกซาเลทได้อีกด้วย การค้นพบนี้อาจให้ข้อมูลสำคัญที่ทำให้เข้าใจกลไกการเกิดโรคนิ่วในไตที่นำไปสู่การสูญเสียการหน้าที่ของไมโครวิลไลบนผิวเซลล์ท่อไตที่พบในผู้ป่าย พร้อมทั้งยังมีประโยชน์ในแง่ของการค้นหาวิธีการรักษาและป้องกันการเกิดโรคนิ่วในไตได้อีกด้วย

คำหลัก : โรคนิ่วในไต, ผลึกแคลเซี่ยมอ๊อกซาเลต, การบาดเจ็บของไมโครวิลไล, การถูกทำลายของเซลล์ท่อไต

1. INTRODUCTION

Calcium oxalate (CaOx) crystal is the potential causative crystal for kidney stone formation and the most common type is calcium oxalate monohydrate (COM) (1). Several theories have been proposed whether the binding of COM crystals onto microvilli of renal tubular epithelial cells is the crucial event initiating kidney stone formation and development (2, 3). Distal and proximal renal tubular epithelial cells which were bound to COM crystals normally showed the evidences of microvilli destruction, transformation of intracellular organelles and intra-tubular aggregation of the collapsed microvilli in rat model (4, 5). The disruption of microvilli and their detachment from apical surface of renal cells are thought to be the major risk factors and can enhance the development of kidney stone in renal tubular lumen (6). Renal tubular epithelial cells are characterized as polarized epithelial cells which their membrane is divided into apical and basolateral membranes to perform specialized transport functions (7). Apical cell surface of renal tubular epithelial cells is covered with microvilli which need some remarkable processes for their proper establishment and maintenance responsible to its potential transport and cell polarity functions (8).

The disruption and loss of microvilli density on apical cell surface is the hallmark of renal tubular cell injury contributing to the development, severity and kidney disease progression (9, 10). Microvillar injuries with evidences of blebbing, sloughing, internalization and decreasing their length and density may be the cause which can initiate renal tubular cell injuries leading to renal tubular epithelial cell dysfunction in kidney stone patients (1, 6). CaOx crystals are injurious to the renal tubular cells by the production of reactive oxygen species (ROS) and also inducing oxidative stress leading to many morphological alterations as well as the destruction of microvilli (6). Nevertheless, the molecular mechanisms in the pathogenesis of microvillar injuries upon COM crystal adhesion have not been evaluated.

In our previous proteomics reports, we found that ezrin which is one of ERM (ezrin, radixin, moesin) protein members and involves in the formation and maintenance of microvilli was changes its protein level in response to COM crystal adhesion (11-13). Ezrin acts as a linker between the cortical plasma membrane and actin cytoskeleton in epithelial cells (8). The dissociation from actin cytoskeleton, the alterations in distribution, localization and posttranslational modification in term of threonine phosphorylation of ezrin can influence its functions and lead to the loss of microvillar structure and density in renal tubular epithelial cells (14-16). In kidney stone disease, the previous studies postulated and recognized the alterations of cellular structure and the damages of microvillar organization both *in vivo* and *in vitro* models in response to oxalate and CaOx crystal administrations (5, 6). Our interest was focused on the

investigation of molecular mechanisms implicating in microvillar injuries and disorganization in response to COM crystal exposure in MDCK cells. The roles of ezrin were examined including the alterations in protein expression, subcellular localization, phosphorylation modifications and its association with actin cytoskeleton. Moreover, roles of EGCG (green tea extract) on protein oxidation and cellular alterations were also investigated. Finally, the findings from this study may provide the important information to enable researchers to discover the novel therapeutic option for preventing and reducing the progression of kidney stone disease.

2. MATERAILS AND METHODS

2.1. Cell culture and COM crystal treatment

Mardin-Darby Canine kidney (MDCK) cells, which represent cells derived from distal/collecting duct tubular epithelial cells, were grown in Eagle's minimum essential medium (MEM) (Gibco; Grand Island, NY) supplemented with 10%heat-inactivated fetal bovine serum (FBS) (Gibco), 1.2%penicillinG/streptomycin (Sigma, St.Louis, MO) and 2 mM of L-glutamine. The cultured cells were maintained in a humidified incubator at 37°C with 5%CO_2 for 24 h. For COM crystal treatment, MDCK cells were seeded for 24 h to obtain 80% confluent monolayer. COM crystals (100 µg/ml) which were resuspended in complete growth medium were added to the cells and incubated for 48 h.

To obtain polarized MDCK monolayer, polycarbonate Transwell inserts (0.4 µm pore size; Corning Costar, Cambridge, MA, USA) were used as culture substrate. MDCK cells at a density of 7.5 X 10^4 cells/ml were split and grown on collagen type IV-coated polycarbonate membrane inserts overnight before COM crystal addition. The collagen type IV-coated polycarbonate membrane insert were prepared by adding of collagen type IV (6 µg/cm^2) (Sigma, St. Louis, MO, USA) solution onto Transwell insert by covering whole surface area and incubated at 4°C overnight.

2.2. Morphological observation

Cell morphology was directly observed under a phase contrast microscope (Olympus CKX41; Tokyo, Japan) after COM crystal treatment for 48 h. Next, the COM crystal-treated MDCK cells were fixed, permeabilized and stained for F-actin cytoskeleton with Oregon Green® 488-conjugated phalloidin for 1 h to detect polymeric F-actin for monitoring the alteration of cell morphology in term of actin cytoskeleton organization after exposure to COM crystals. After washing, the stained cells were mounted in 50%glycerol in PBS on glass slide. The XY, XZ and YZ sections of these cells were acquired by using a Nikon A1R laser scanning confocal microscope (Nikon Instruments, Inc., New York, United States).

2.3. Determination of expression level of ezrin after COM crystal treatment by Western blot analysis

After COM crystal treatment for 48 h, MDCK cells were extracted in 1XLaemmli's buffer and protein lysate was separated by SDS-PAGE. The resolved proteins were transferred onto a nitrocellulose membrane. Then, the nitrocellulose membrane was blocked non-specific bindings by 5%skim milk in PBS and incubated with primary antibody specific to ezrin overnight at 4°C.

The corresponding secondary antibody conjugated with horseradish peroxidase (HRP) was used to detect and the immunoreactive band was visualized by using SuperSignal West Pico chemiluminescence substrate (Pierce Biotechnology, Inc., Rockford, IL) and then exposed to X-ray film.

2.4. Determination of the alteration in subcellular localization and distribution of ezrin after COM crystal treatment

2.4.1 Alteration in apical membrane association

To determine the alteration in apical/brush border association of ezrin, apical membrane of MDCK cells was isolated after COM crystal treatment using a peeling protocol as we previously described (17). Briefly, COM crystal-treated MDCK cells were rinsed twice with ice-cold PBS^{+} (special containing 1 mM $MgCl_2$ and 0.1 mM $CaCl_2$) and then the solution was extremely aspirated. Whatman filter paper (Whatman®, Whatman International Ltd., Maidstone, England) was used to isolate the apical membrane of the cells. The filter paper was prewetted with deionized water and then placed on the cell monolayer. After waiting for 5 min, the filter paper was quickly removed. The isolated apical membrane was allowed to release from filer paper in deionized water. The isolated apical membrane-enriched solution was concentrated by lyophilization and then solubilized in 1XLaemmli's buffer. Western blotting was performed to determine the change of ezrin expression in the apical membrane of MDCK cells after COM crystal exposure.

2.4.2 Alteration in actin cytoskeleton association

To examine the effect of COM crystal adhesion on the association with actin cytoskeleton of ezrin, Triton X-100 solubility assay and Western blot analysis were applied. After COM crystal treatment, the cells were briefly rinsed with buffer containing 10 mM Tris-HCL (pH 7.5), 150 mM NaCl. Then, cells were extracted in buffer containing 0.5%Triton X-100, 10 mM Tris-HCL (pH 7.5), 100 mM NaCl and 300 mM sucrose for 15 min at 4°C. The Triton X-100 soluble (non-cytoskeleton) and insoluble (cytoskeleton and cytoskeleton-associated proteins) fractions were analyzed by Western blot analysis.

2.4.3 Alteration in localization and distribution of ezrin using laser scanning confocal microscope

After treatment with COM crystals, MDCK cells were processed for confocal microscopic examination to visualize the change of localization and distribution of ezrin. The COM crystal-treated cells were fixed with 3.7%paraformaldehyde for 15 min and then permeabilized with 0.1%Triton X-100 for 15 min. Then, the cells were incubated with anti-ezrin primary antibody and followed by fluorescence dye-conjugated corresponding secondary antibody. The stained

cells were observed and confocal images were acquired by laser scanning confocal microscope according to the protocol as describe above.

2.5. Determination of posttranslational modification (phosphorylation) of ezrin after COM crystal treatment

To determine the change in threonine phosphorylation modification of ezrin after COM crystal treatment, immunoprecipitation (18) and Western blotting were performed. Control and COM crystal-treated MDCK cells were extracted in RIPA buffer (25 mM Tris-HCl, pH 7.6, 150 mM NaCl, 1%NP-40, 1%sodium deoxycholate and 0.1%SDS) and then protein concentration was estimated by Bradford's protein assay (19). An equal protein amount (1 mg) from each condition was incubated with anti-phosphothreonine (1 µg) for overnight at 4°C on rotator. Protein G-Sepharose beads were added into protein solution and then further incubated for 4 h 4°C on rotator. After three washing with lysis buffer (50 mM Tri-HCl, pH 7.4, 150 mM NaCl, 0.5%Triton X-100 and 1 mM EDTA), threonine-phosphorylated proteins were collected by incubating with 30 µl of 1XLaemmli's buffer and then heated at 95°C for 5 min. IP eluates from each condition were resolved by SDS-PAGE and then blotted onto nitrocellulose membrane. Anti-ezrin antibody was used to determine the alteration of ezrin level in phosphothreonine-containing proteins in response to COM crystal adhesion.

2.6. Alterations in microvilli density of renal tubular epithelial cells after COM crystal treatment

After COM crystal treatment for 48 h, control and crystal-treated MDCK cells were washed three times with PBS^{+}. Both cells were then fixed by 3.7%paraformaldehyde and permeabilized by 0.1%Triton X-100 in PBS. After washing with PBS, the cells were stained for F-actin with Oregon Green® 488-conjugated phalloidin for 1 h to detect polymeric F-actin and further observed under confocal microscope. The stained cells were mounted in 50%glycerol in PBS on glass slide and images were acquired by using a Nikon A1R confocal microscope (Nikon Instruments, Inc., New York, United States).

2.7. Epigallocatechin-3-gallate (EGCG) pretreatment and protein oxidation determination after COM crystal exposure

EGCG was used as an antioxidant chemical to reduce level of protein oxidation resulting from COM crystal treatment in MDCK cells. MDCK cells were seeded and grown overnight in CO_2 incubator to obtain 80% confluent monolayer. Growth medium was removed and then the

cells were incubated with 25 μM of EGCG for 30 min. Thereafter, COM crystals (100 μg/ml) were added to the cells and further incubated for 48 h in CO_2 incubator at 37°C.

The level of protein oxidation determination was performed using the manufacturer's guideline from OxyBlot™ Protein Oxidation Detection Kit protocol (Chemicon, Inc., Temecula, CA). First, an equal amount of protein from control and COM crystal-treated cells was subjected to derivatization carbonyl groups which are represented the oxidative damage to a protein by a 2, 4-dinitrophenyl-hydrazone (DNP) moiety. Next, these derivatized proteins were resolved on 12%SDS-PAGE gel and then blotted onto nitrocellulose membranes. The membrane was block non-specific binding with 5%BSA in PBS for 30 min and then incubated with rabbit anti-DNPH antibody to detect the oxidative modified proteins. After washing, the membrane was further exposed to corresponding HRP-conjugated secondary antibody. Finally, membrane was washed twice in washing buffer (PBS containing 0.2%Tween-20). Protein bands were visualized by using SuperSignal West Pico chemiluminescence substrate and then exposed to X-ray film. Band signal intensity was measured by ImageMaster 2D Platinum software.

2.8. Statistical analysis

The data was shown as mean ± SEM. Comparisons among groups were analyzed by unpaired Student's *t* test and one-way analysis of variance (ANOVA) with Tukey's posthoc test (SPSS; version 13.0). *P*-values less than 0.05 were considered statistically significant.

3. RESULTS

3.1. COM crystal adhesion induces morphological changes in MDCK cells

MDCK cells were seeded and divided into control (without COM crystal treatment) and COM crystal-treated groups. COM crystals (100 μg/ml) were added into complete growth medium and then vigorously mixed before adding to the cells. After 48 h of incubation, examination of cell morphology under phase contrast microscope showed the striking morphological change in COM crystal-treated cells compared to control cells (**Figure 1**). COM crystal-treated MDCK cells showed the highly irregular shape with poorly intact monolayer. We next explored the morphological changes of MDCK cells after COM crystal treatment by determining the distribution and organization of F-actin cytoskeleton. In control MDCK cells, F-actin was stained with similar intensity along the apical (microvilli) and lateral membranes of the cells. In COM crystal-treated MDCK cells, F-actin was obviously reduced in the intensity of apical staining but concentrated along the lateral and basal membranes which clearly show in vertical (XY) and horizontal (XZ) sections of confocal images (**Figure 2**).

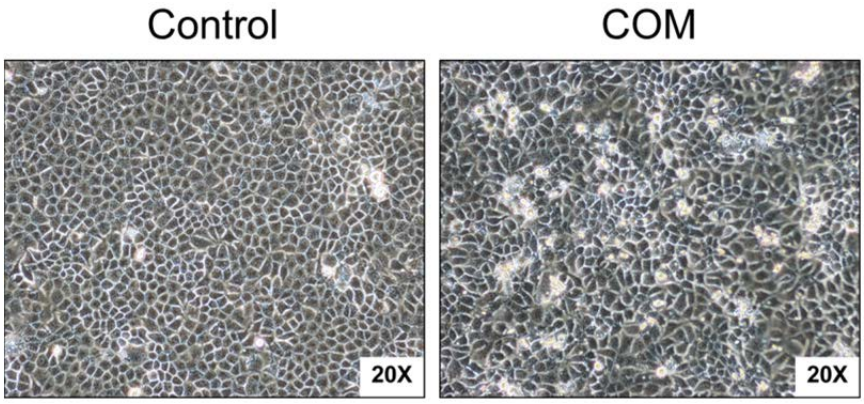

Figure 1. Phase contrast images of MDCK cells grown in the absence (control) or presence of COM crystals (100 μg/ml) for 48 h. Original magnification is 200X.

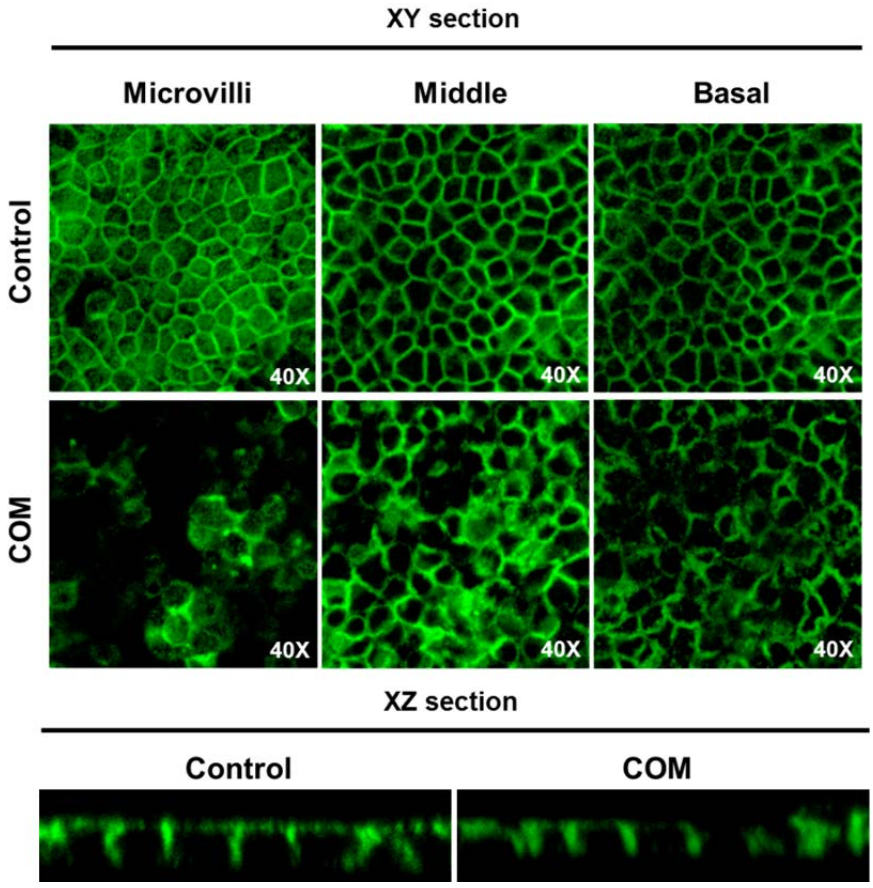

Figure 2. Distribution and organization of F-actin in control and COM crystal-treated MDCK cells were shown by confocal microscopy (XY and XZ sections). Cells were grown on polycarbonate filters in Transwell insert in the absence and presence of COM crystals (100 μg/ml) for 48 h and F-actin was stained with Oregon Green® 488-conjugated phalloidin and shown in green signal. Original magnification is 400X.

3.2. Microvilli density at apical surface of MDCK cells was decreased after COM crystal treatment

It is well known that microvilli consist of a core of bundled actin filaments and were consistent with the apical F-actin staining pattern. Thus, we stained MDCK cells with Oregon Green® 488-conjugated phalloidin to stain F-actin and explore the alteration of microvilli density at the apical surface of MDCK cells after COM crystal treatment. Microvilli covering the apical surface of control and COM crystal-treated cells were observed under laser scanning confocal microscope which provides high resolution and high magnification images. The result showed that COM crystal-treated MDCK cells exhibited lower apical F-actin levels and loss of its normal staining pattern suggesting the decreasing of apical microvilli density after COM crystal treatment.

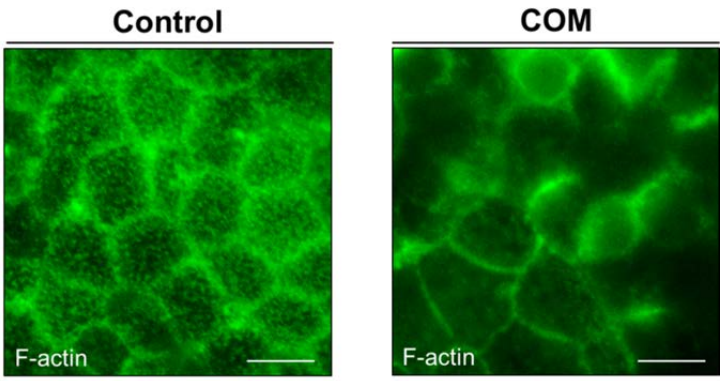

Figure 3. Microvilli which covering the apical surface of control and COM crystal-treated MDCK cells was visualized by phalloidin-labeled F-actin using laser scanning confocal microscopy (scale bar = 10 μm).

3.3. Expression of ezrin was decreased in COM crystal-treated MDCK cells

To determine whether expression level of ezrin in whole cell lysate was altered after COM crystal treatment, Western blotting was performed. The result showed in **Figure 4** demonstrated that approximately 82 kDa band of ezrin in COM crystal-treated cell lysate was obviously decreased when compared to control cell lysate (**Figure 4A**). The ezrin band intensities were quantified using ImageMaster 2D Platinum software and the relative band intensity of ezrin was obtained by normalizing with band intensity of GAPDH (**Figure 4B**). The results indicated that there was a significant decrease in ezrin level which occurred during COM crystal treatment.

(A)

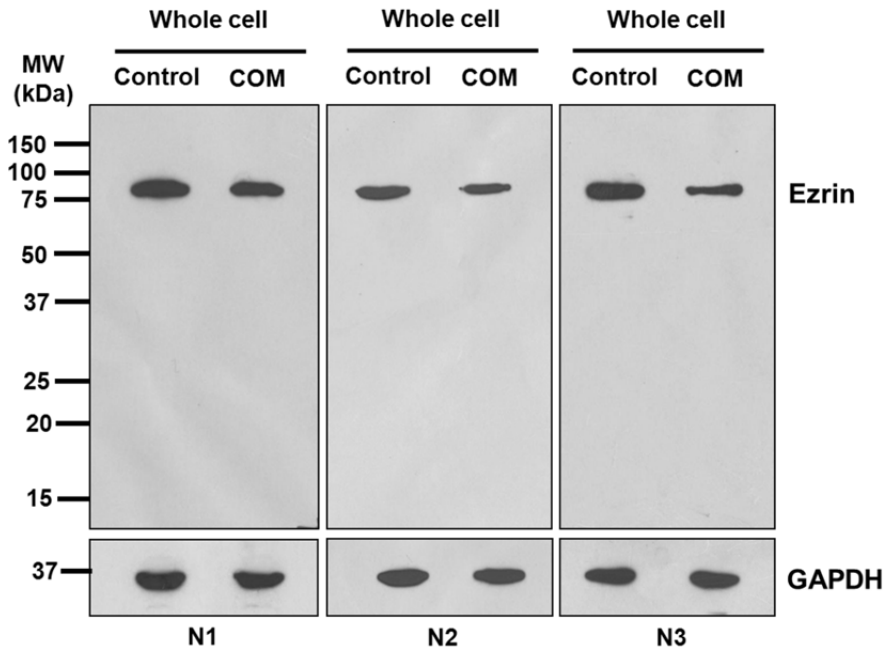

(B)

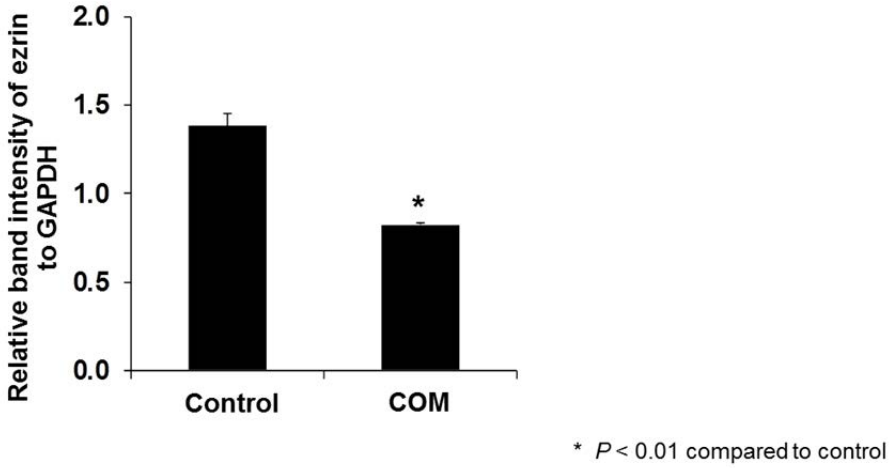

Figure 4. Western blot analysis of ezrin in whole cell lysate extracted from control and COM crystal-treated MDCK cells (n = 3) (**A**). Relative band intensity of ezrin was normalized to GAPDH for each individual and the data are presented as mean ± SEM (**B**). GAPDH was used as a loading control. *P*-values less than 0.05 were considered statistically significant.

3.4. Apical membrane expression of ezrin and actin cytoskeleton was decreased in COM crystal-treated MDCK cells

To investigate the effects of COM crystals on the distribution and localization of ezrin and F-actin cytoskeleton, immunofluorescence staining and confocal microscopy were applied. In control cells, ezrin was highly concentrated at the apical membrane whereas F-actin was concentrated in both apical and lateral membranes of the cells as shown in **Figure 5A** and **Figure 6A**, respectively. In contrast, COM crystal-treated MDCK cells showed a striking decrease of ezrin and F-actin which localized at the apical membrane of cell monolayer (**Figure 5A** and **Figure 6A**). To further confirm the immunofluorescence data indicating a decrease in apical localization of ezrin and F-actin, we then isolated apical membrane of control and COM crystal-treated monolayer by peeling method using filter paper. The isolated apical membrane from both conditions were solubilized in 1XLaemmli's buffer and then an equal amount of apical membrane protein from control and crystal-treated cells were processed by Western blotting in parallel with cytosolic fraction (the remaining part of cell monolayer after apical peeling). The nitrocellulose membrane was probed with anti-ezrin and anti-β-actin antibodies, respectively. Western blot data showed that ezrin and β-actin levels were selectively decreased only in apical membrane isolated from COM crystal-treated cells (**Figure 5B** and **Figure 6B**) whereas ezrin expression in the cytosolic (the remaining part of monolayer after apical peeling) fraction was not changed.

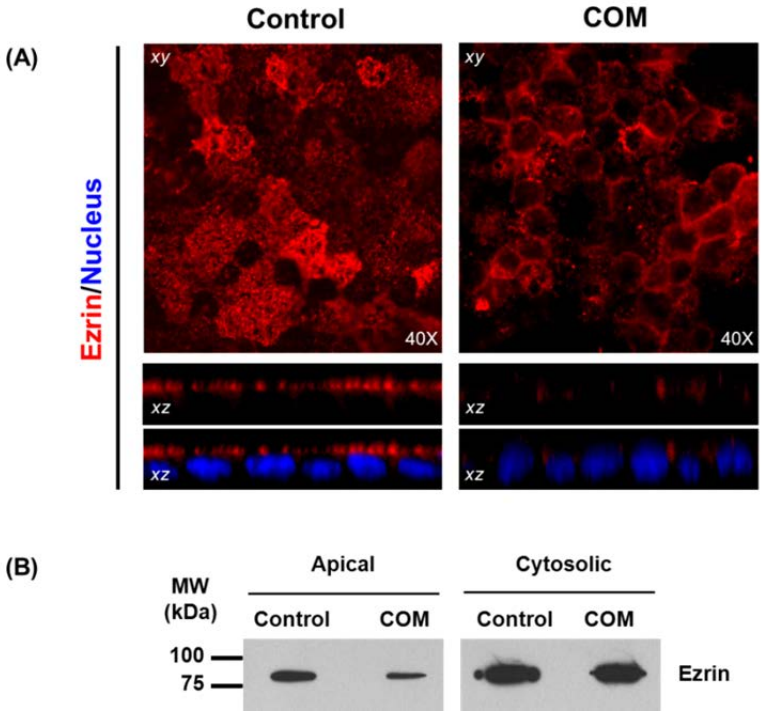

Figure 5. Localization and distribution of ezrin in control and COM crystal-treated MDCK cells under laser scanning confocal microscope (**A**). Cells were grown on polycarbonate filters in the absence (control) and presence of COM crystals (100 µg/ml) for 48 h. Ezrin was shown in red and nucleus was stained by Hoechst dye and presented in blue signal. Original magnification is 400X. (**B**) Western blot analysis of ezrin in apical membrane and cytosolic fractions extracted from control and COM crystal-treated MDCK cells.

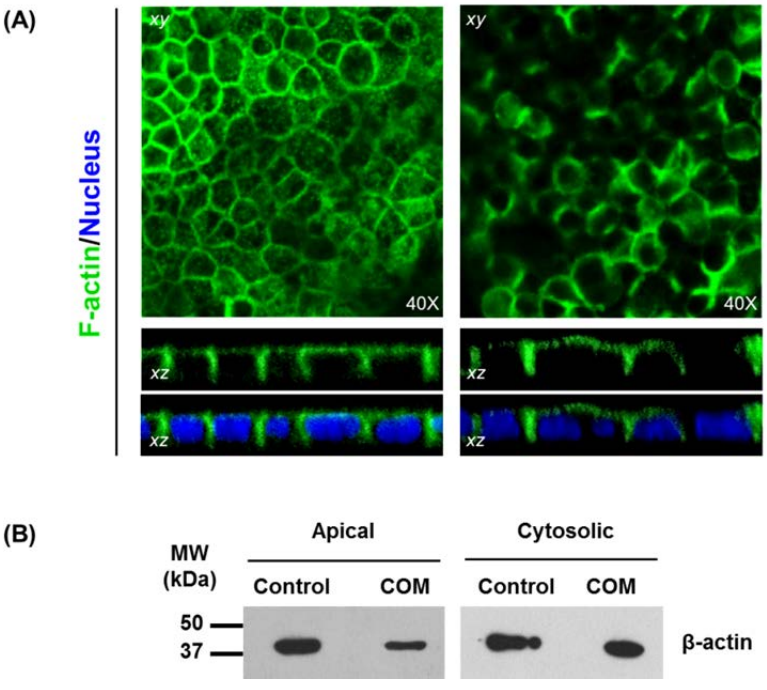

Figure 6. Distribution and organization of F-actin cytoskeleton in control and COM crystal-treated MDCK cells as shown by confocal microscopy (**A**). Cells were grown on polycarbonate filters in the absence (control) and presence of COM crystals (100 μg/ml) for 48 h. F-actin cytoskeleton was stained with Oregon Green® 488-conjugated phalloidin and shown in green signal. Nucleus was stained by Hoechst dye and shown in blue signal. Original magnification is 400X. (**B**) Western blot analysis of β-actin in apical membrane and cytosolic fractions extracted from control and COM crystal-treated MDCK cells.

3.5. Alteration of ezrin localization and its relation with actin cytoskeleton after COM crystal treatment

We further investigated the effect of COM crystal on the association of ezrin to actin cytoskeleton which could refer to alteration of functional ezrin. Selective detergent extraction which was commonly used to isolate cytoskeleton and cytoskeleton-associated proteins was applied by incubating the cells with 0.5%Triton X-100-containinig buffer to obtain cytoskeleton including cytoskeleton-associated proteins (Triton X-100-insoluble) and non-cytoskeleton (Triton X-100-soluble) fractions. Western blot data showed the distribution of ezrin in both fractions of control and COM crystal-treated cells. We found the decreasing of ezrin in cytoskeleton fraction (Triton X-100-insoluble) in COM crystal-treated cells (**Figure 7**) referring to the decreasing of functional ezrin pool in COM crystal-treated cells. Confocal images also presented the loss of apical ezrin which clearly showed in XZ-scanned sections (**Figure 8**). Likewise, the confocal data revealed the interesting observation which we found mislocalization of the remaining ezrin concentrated along the lateral border of COM crystal-treated cells (**Figure 8C**). Because active or functional ezrin is normally associated with actin cytoskeleton and mainly present at apical membrane of epithelial cells, we next isolated apical membrane of control and COM crystal-treated cells and then extracted with 0.5%Triton X-100-containing buffer. Western blot data showed a selective decreased of ezrin and F-actin only in apical membrane which again implying the reduction of functional ezrin was observed after COM crystal treatment (**Figure 9**).

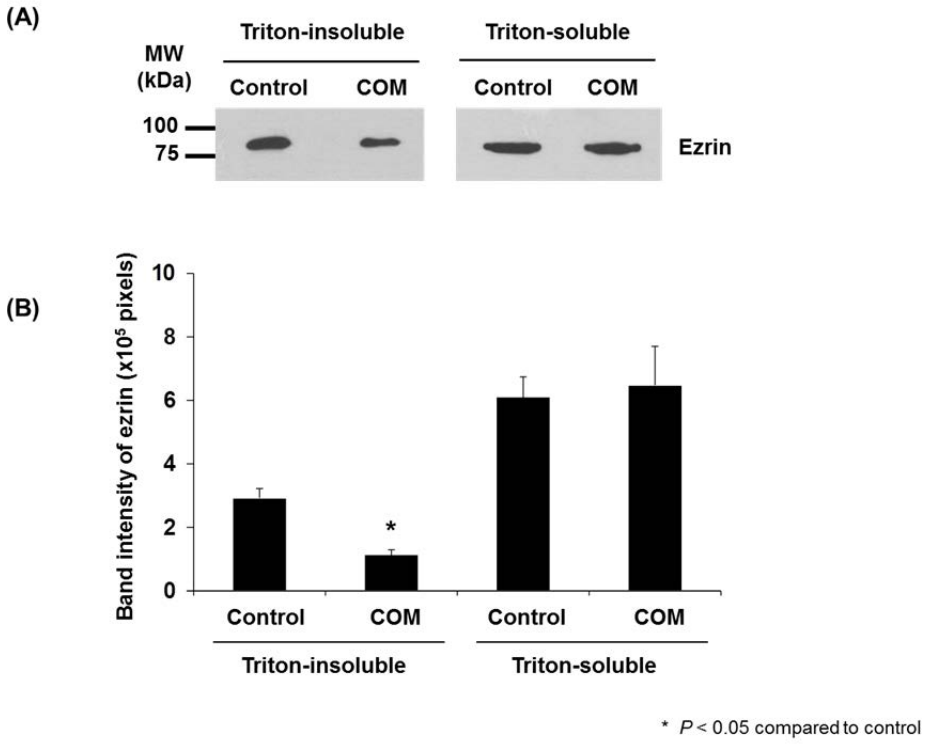

Figure 7. Distribution of ezrin in cytoskeleton and non-cytoskeleton fractions obtained by Triton X-100 extraction from control and COM crystal-treated MDCK cells (n = 3) (**A**). Band intensity of ezrin was quantified and the data are presented as mean ± SEM (**B**). *P*-values less than 0.05 were considered statistically significant.

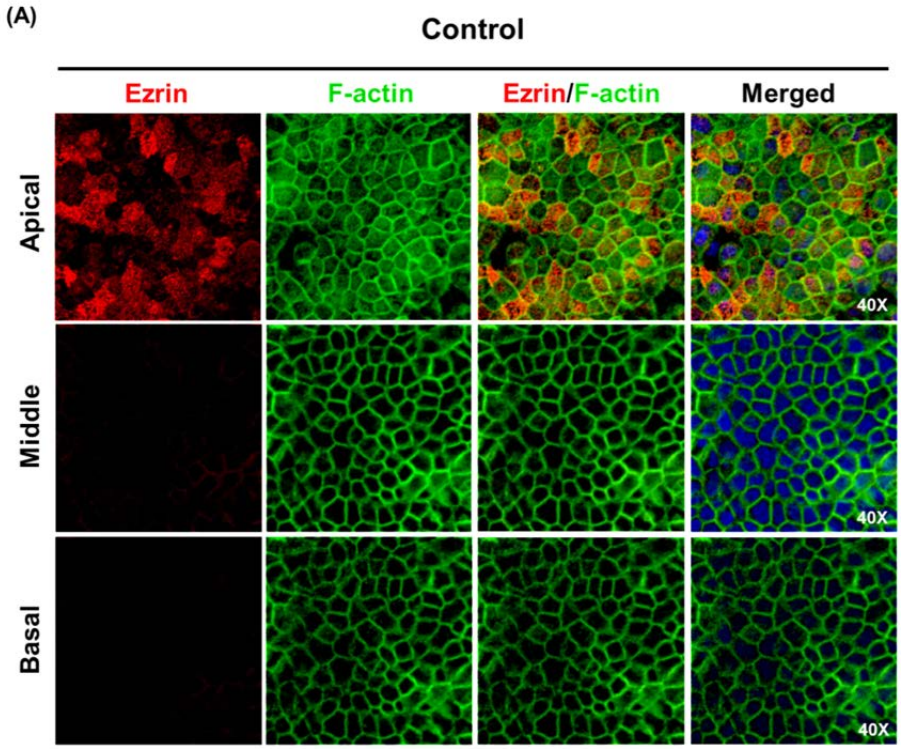

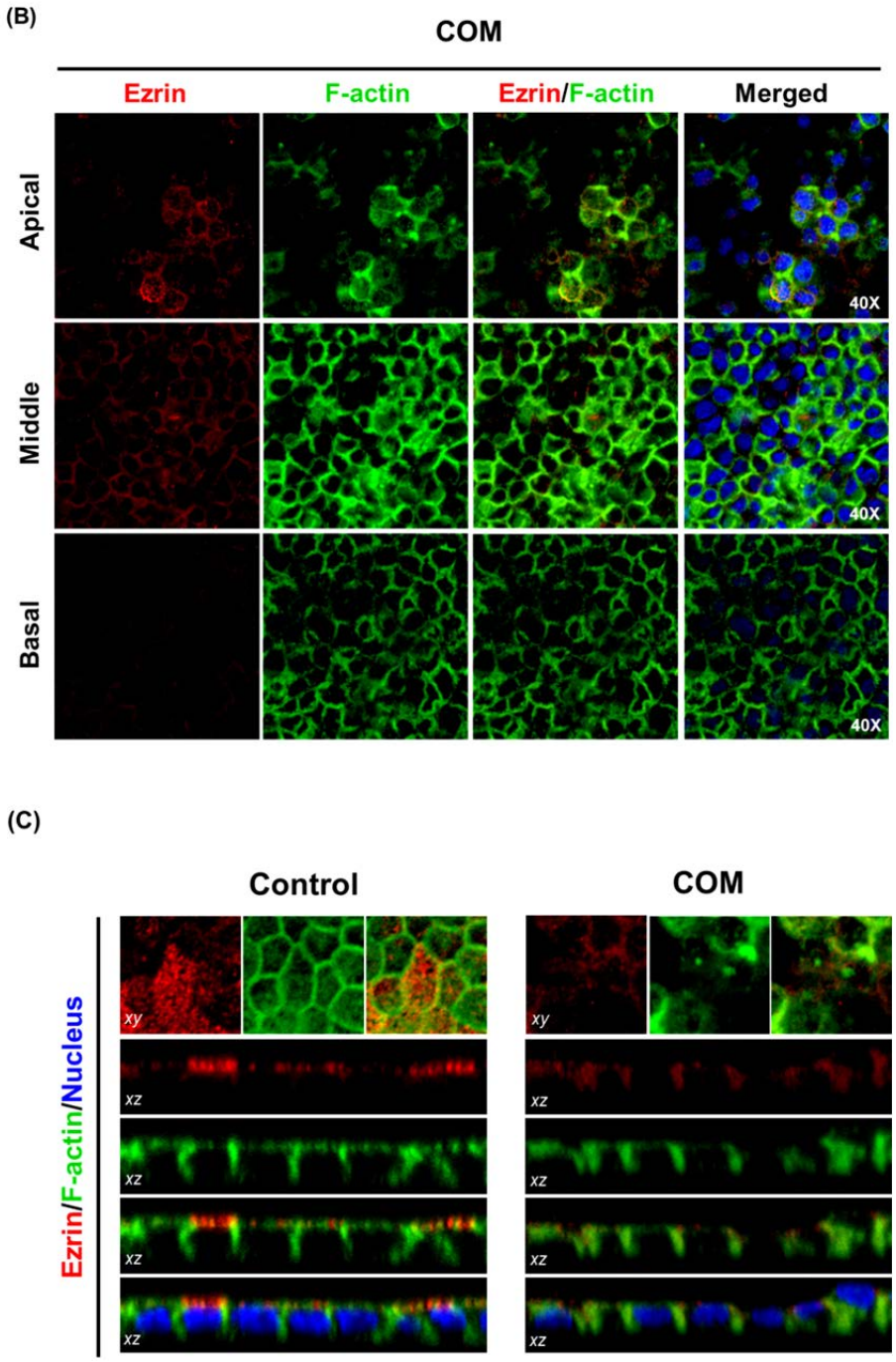

Figure 8. Distribution and colocalization of ezrin and F-actin in different serial focal planes from apical to basal of control (**A**) and COM crystal-treated MDCK cells (**B**). XZ sections of images from each condition was illustrated in **C**. Ezrin was presented in red signal and F-actin was stained with Oregon Green® 488-conjugated phalloidin and presented in green signal. Nuclei of the cells were stained by Hoechst dye and shown in blue signal. Original magnification is 400X.

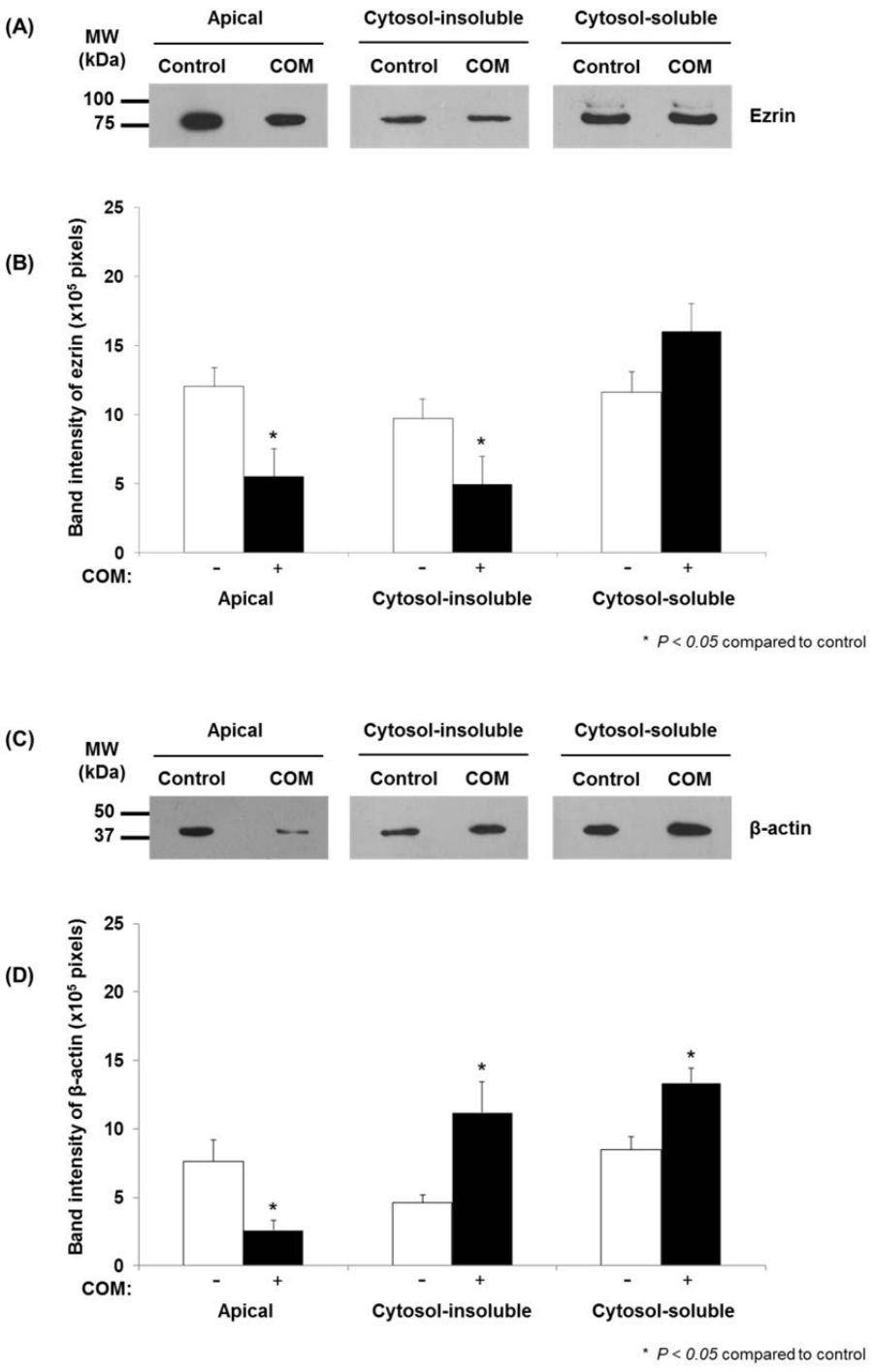

Figure 9. Western blot analysis of ezrin (**A**) and β-actin (**C**) in the isolated apical membrane fraction, cytoskeleton and non-cytoskeleton fractions which were extracted after apical peeling from control and COM crystal-treated MDCK cells (n = 3). Band intensity of ezrin (**B**) and β-actin (**D**) were quantified and the data are presented as mean ± SEM. *P*-values less than 0.05 were considered statistically significant.

3.6. Threonine-phosphorylated ezrin is increased in COM crystal-treated MDCK cell lysate

Phosphorylation is one of the main processes which can determine functional ezrin. The entire sequence of dog ezrin was subjected to predict number of potential phosphoresidues using NetPhos 2.0 software (http://www.cbs.dtu.dk/services/NetPhos/) (20). The result showed many potential phosphoresidues including serine (12 residues), threonine (10 residues) and tyrosine (7 residues) were predicted and presented in **Figure 10**. Because the phosphorylation on threonine residues seems to play role in ezrin function, we next evaluated whether level of threonine phosphorylation of ezrin was altered by performing immunoprecipitation with anti-phosphothreonine and then immunoblotting with anti-ezrin antibodies. Whole cell extracts were prepared from control and COM crystal-treated MDCK cells and protein concentrations were quantified according to Bradford's protocol (19). Immunoprecipitation was done by adding anti-phosphothreonine antibody to protein aliquot of control and COM crystal-treated whole cell lysates, separately. After immunoblotting using anti-ezrin antibody, we found that large amount of ezrin could be detected in the immunoprecipitate prepared from COM crystal-treated cells (**Figure 11**). Interestingly, ezrin is normally detected at ~80 kDa in control MDCK cell lysate, but we found two additional upper bands of ezrin (phosphorylated form) were increased in COM crystal-treated cells suggesting the increasing of posttranslationally modified (phosphorylation) of ezrin under COM crystal-treated condition.

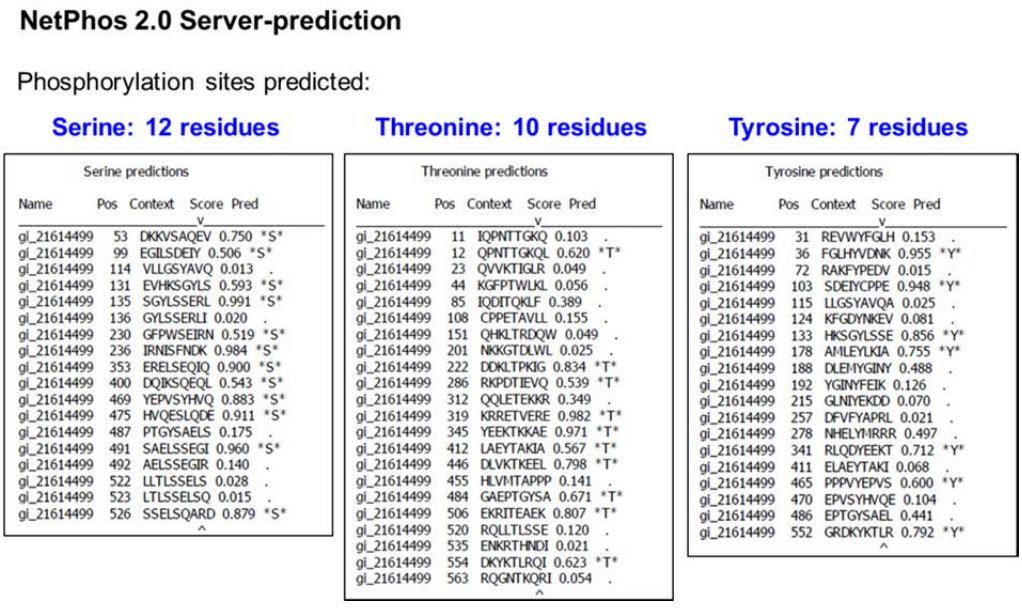

NetPhos 2.0 Server-prediction

Phosphorylation sites predicted:

Serine: 12 residues

Serine predictions

Name	Pos	Context	Score	Pred
gi_21614499	53	DKKVSAQEV	0.750	*S*
gi_21614499	99	EGILSDEIY	0.506	*S*
gi_21614499	114	VLLGSYAVQ	0.013	.
gi_21614499	131	EVHKSGYLS	0.593	*S*
gi_21614499	135	SGYLSSERL	0.991	*S*
gi_21614499	136	GYLSSERLI	0.020	.
gi_21614499	230	GFPWSEIRN	0.519	*S*
gi_21614499	236	IRNISFNDK	0.984	*S*
gi_21614499	353	ERELSEQIQ	0.900	*S*
gi_21614499	400	DQIKSQEQL	0.543	*S*
gi_21614499	469	YEPVSYHVQ	0.883	*S*
gi_21614499	475	HVQESLQDE	0.911	*S*
gi_21614499	487	PTGYSAELS	0.175	.
gi_21614499	491	SAELSSEGI	0.960	*S*
gi_21614499	492	AELSSEGIR	0.140	.
gi_21614499	522	LLTLSSELS	0.028	.
gi_21614499	523	LTLSSELSQ	0.015	.
gi_21614499	526	SSELSQARD	0.879	*S*

Threonine: 10 residues

Threonine predictions

Name	Pos	Context	Score	Pred
gi_21614499	11	IQPNTTGKQ	0.103	.
gi_21614499	12	QPNTTGKQL	0.620	*T*
gi_21614499	23	QVVKTIGLR	0.049	.
gi_21614499	44	KGFPTWLKL	0.056	.
gi_21614499	85	IQDITQKLF	0.389	.
gi_21614499	108	CPPETAVLL	0.155	.
gi_21614499	151	QHKLTRDQW	0.049	.
gi_21614499	201	NKKGTDLWL	0.025	.
gi_21614499	222	DDKLTPKIG	0.834	*T*
gi_21614499	286	RKPDTIEVQ	0.539	*T*
gi_21614499	312	QQLETEKKR	0.349	.
gi_21614499	319	KRRETVERE	0.982	*T*
gi_21614499	345	YEEKTKKAE	0.971	*T*
gi_21614499	412	LAEYTAKIA	0.567	*T*
gi_21614499	446	DLVKTKEEL	0.798	*T*
gi_21614499	455	HLVMTAPPP	0.141	.
gi_21614499	484	GAEPTGYSA	0.671	*T*
gi_21614499	506	EKRITEAEK	0.807	*T*
gi_21614499	520	RQLLTLSSE	0.120	.
gi_21614499	535	ENKRTHNDI	0.021	.
gi_21614499	554	DKYKTLRQI	0.623	*T*
gi_21614499	563	RQGNTKQRI	0.054	.

Tyrosine: 7 residues

Tyrosine predictions

Name	Pos	Context	Score	Pred
gi_21614499	31	REVWYFGLH	0.153	.
gi_21614499	36	FGLHYVDNK	0.955	*Y*
gi_21614499	72	RAKFYPEDV	0.015	.
gi_21614499	103	SDEIYCPPE	0.948	*Y*
gi_21614499	115	LLGSYAVQA	0.025	.
gi_21614499	124	KFGDYNKEV	0.081	.
gi_21614499	133	HKSGYLSSE	0.856	*Y*
gi_21614499	178	AMLEYLKIA	0.755	*Y*
gi_21614499	188	DLEMYGINY	0.488	.
gi_21614499	192	YGINYFEIK	0.126	.
gi_21614499	215	GLNIYEKDD	0.070	.
gi_21614499	257	DFVFYAPRL	0.021	.
gi_21614499	278	NHELYMRRR	0.497	.
gi_21614499	341	RLQDYEEKT	0.712	*Y*
gi_21614499	411	ELAEYTAKI	0.068	.
gi_21614499	465	PPPVYEPVS	0.600	*Y*
gi_21614499	470	EPVSYHVQE	0.104	.
gi_21614499	486	EPTGYSAEL	0.441	.
gi_21614499	552	GRDKYKTLR	0.792	*Y*

Figure 10. The potential phosphorylation sites of ezrin were predicted using NetPhos 2.0 software. Numbers of predicted phosphoserine, phosphothreonine and phosphotyrosine residues were presented, respectively.

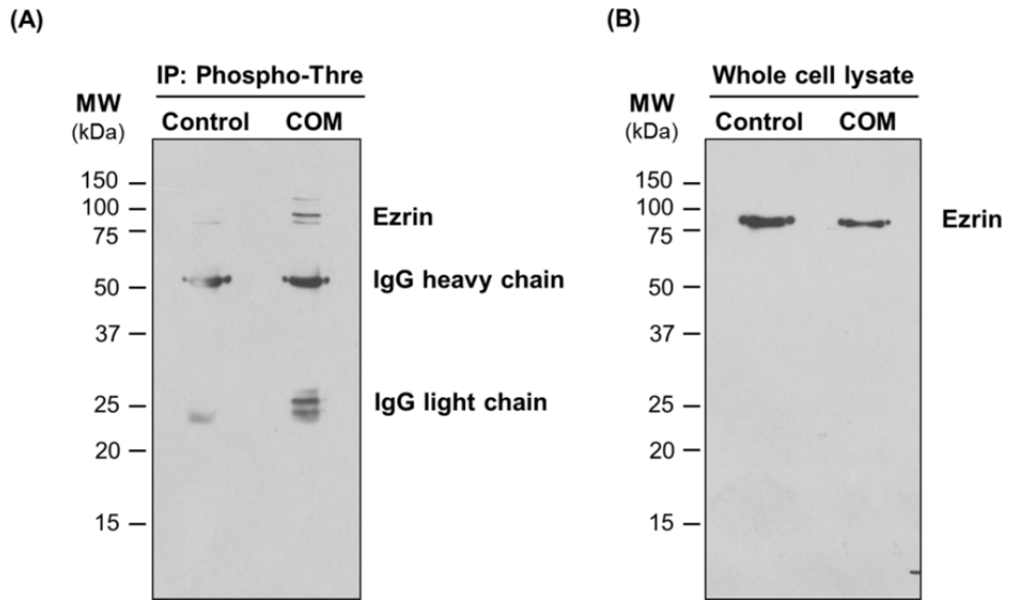

Figure 11. Western blot analysis of ezrin in IP eluates (**A**) and whole cell lysate (**B**) extracted from control and COM crystal-treated MDCK cells. Level of ezrin in threonine-phosphorylated pool was increased and decreased in whole cell lysate which was extracted from COM crystal-treated MDCK cells.

3.7. Protein oxidation level was increased in response to COM crystal treatment

Many previous studies showed the induction of oxidative stress by increasing of reactive oxygen species production which can cause extensive oxidative damage to proteins in response to CaOx crystal adhesion of renal cells (6, 21, 22). In this study, we determined whether level of protein oxidation was increased in MDCK cells after COM crystal treatment by detecting level of protein carbonylation (the end production of protein oxidation) using OxyBlot assay. Protein oxidation may be the cause of ezrin degradation resulting in the decreasing of ezrin level after COM crystal treatment. The results showed that the statistically significant increase in protein carbonylation was found in protein lysate extracted from COM crystal-treated cells (**Figure 12**) indicating the induction of protein oxidation causes by COM crystal treatment.

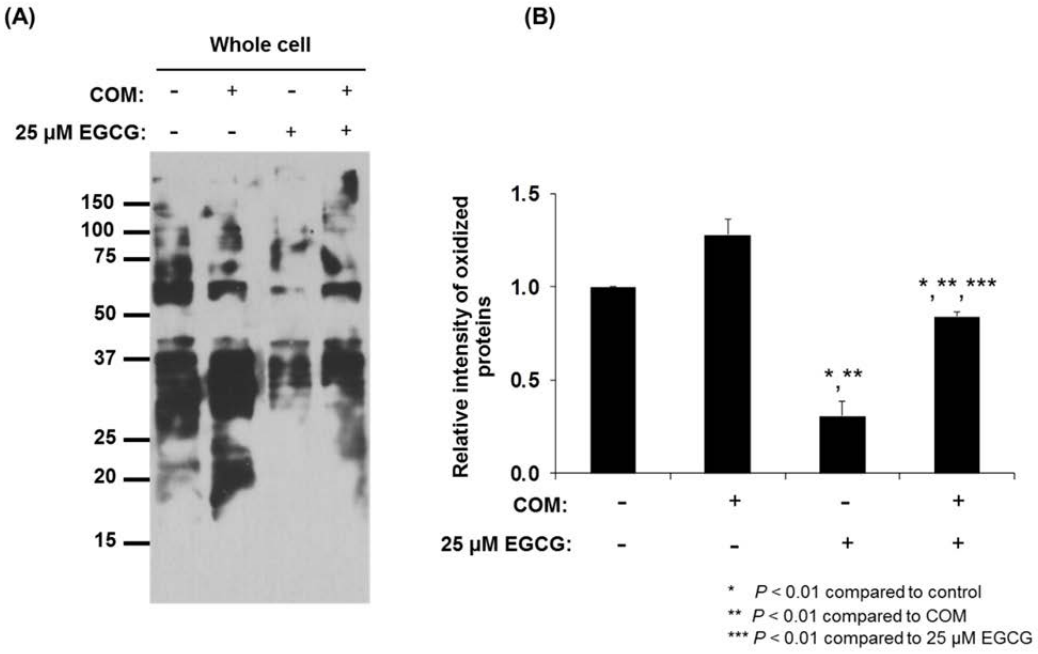

Figure 12. OxyBlot analysis of control and COM crystal-treated MDCK cells with or without 25 μM of EGCG pretreatment (**A**). Relative band intensity of oxidized proteins normalized to control condition was quantified and the data are presented as mean ± SEM (n = 3) (**B**). *P*-values less than 0.05 were considered statistically significant.

3.8. EGCG pretreatment can completely prevent the increasing of protein oxidation and the decreasing of ezrin expression during COM crystal treatment

From our data, we demonstrated the increasing of protein oxidation level in COM crystal-treated MDCK cells which could be the cause of ezrin degradation. Next, we used an antioxidant epigallocatechin-3-gallate (EGCG) which is extracted from green tea and has strong antioxidative activity to reduce protein oxidation during COM crystal treatment. MDCK cells were pretreated with 25 μM of EGCG for 30 min before adding 100 μg/ml of COM crystals for 48 h. We found the reduction of protein oxidation level in control cells which were pretreated with EGCG as shown in **Figure 12**. As expected, EGCG pretreatment can protect the cells from oxidative stress during COM crystal treatment by significantly decrease the level of protein oxidation (**Figure 12**). And the use of EGCG can also prevent the reduction of ezrin expression level during COM crystal treatment as indicated in **Figure 13**.

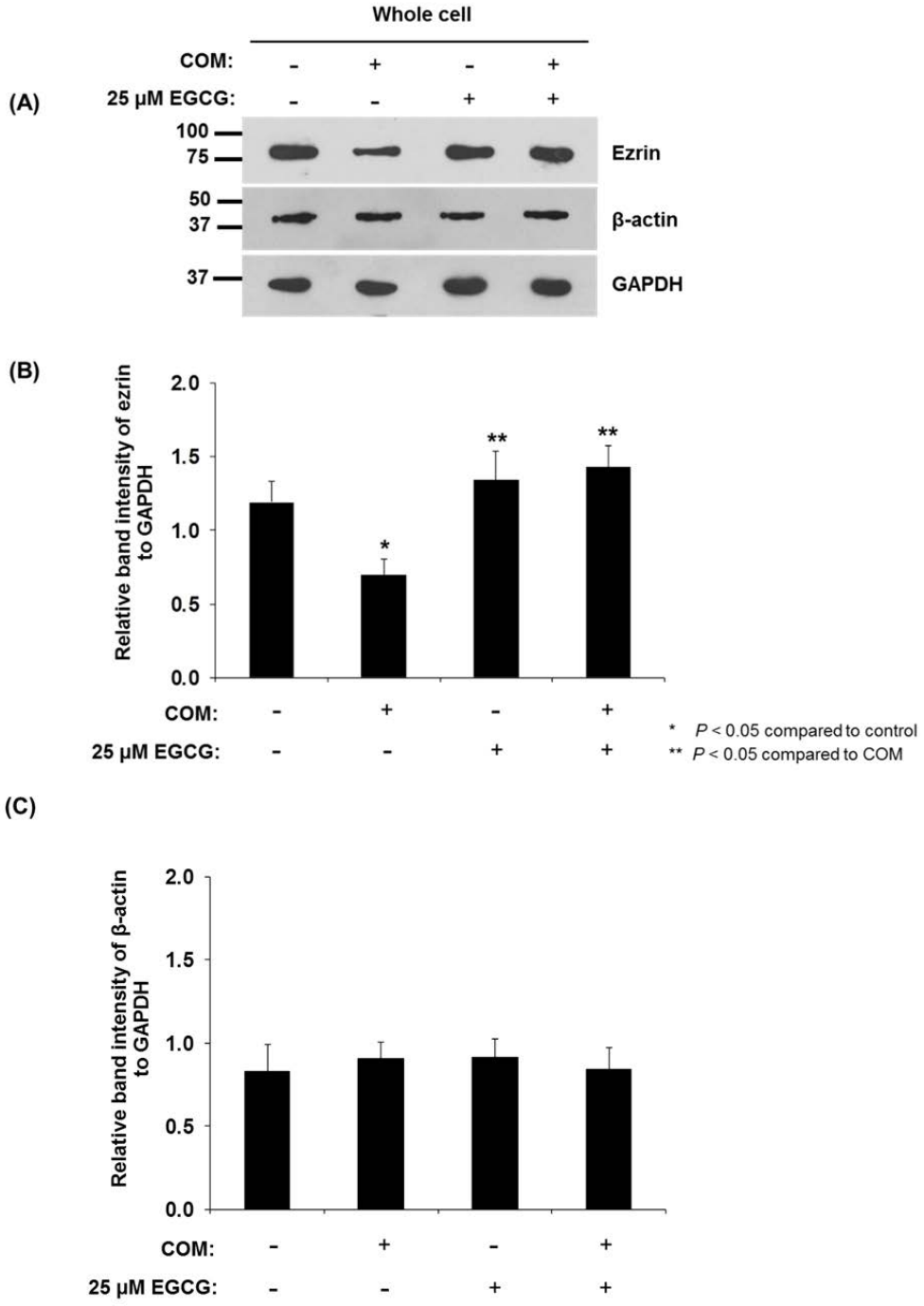

Figure 13. Western blot analysis of ezrin and β-actin in whole cell lysate extracted from control and COM crystal-treated MDCK cells with or without 25 μM of EGCG pretreatment (**A**). Relative band intensities of ezrin and β-actin to GAPDH were quantified and the data are presented as mean ± SEM (n = 3) (**B** and **C**). *P*-values less than 0.05 were considered statistically significant.

3.9. EGCG pretreatment can partially protect the decreasing of apical ezrin and actin cytoskeleton in response to COM crystal treatment

As our data show that pretreatment MDCK cells by EGCG can prevent the reduction of ezrin expression level by decreasing protein oxidation level after COM crystal treatment. We also used EGCG to pretreat the cells and then further examined its effect on the stabilization of apical ezrin and actin cytoskeleton during COM crystal treatment. EGCG pretreatment showed a nearly complete protection of the loss of apical ezrin and F-actin expression and localization against COM crystal treatment (**Figure 14**).

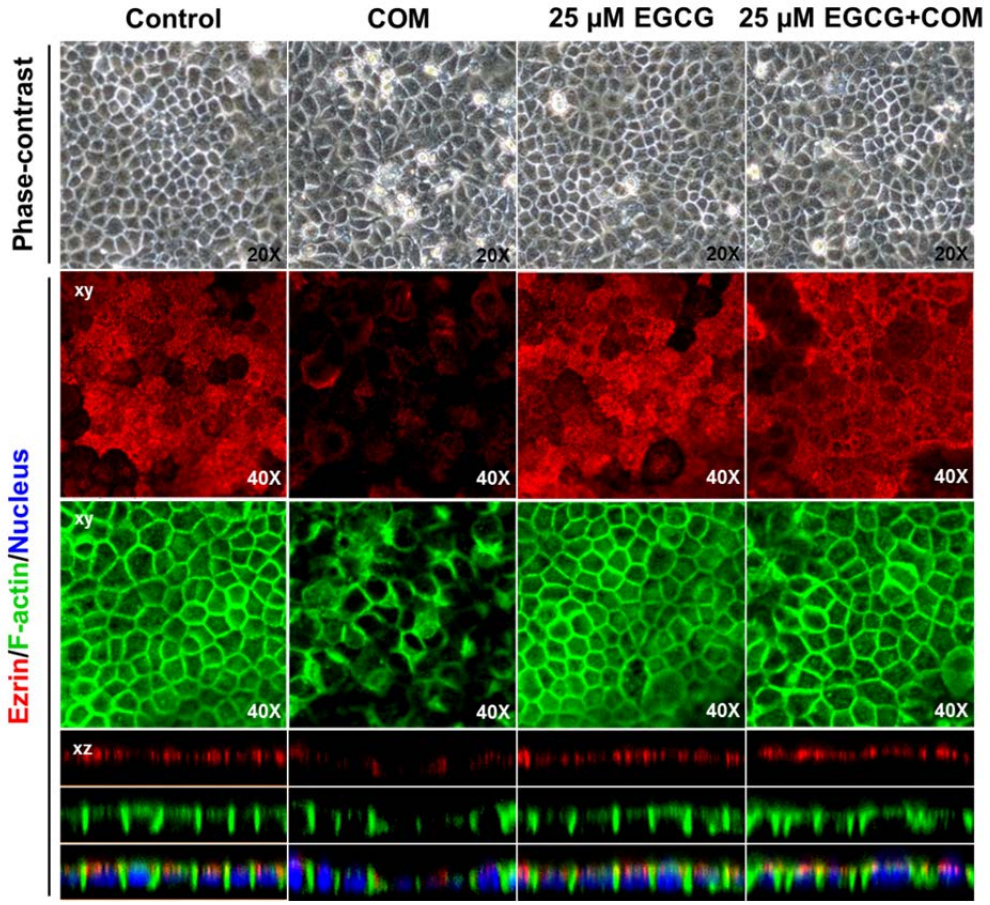

Figure 14. Protective effect of EGCG pretreatment on the decreasing of apical ezrin and actin cytoskeleton in response to COM crystal adhesion. Pretreatment MDCK cells with 25 μM of EGCG for 30 min before adding COM crystals (100 μg/ml) for 48 h can partially prevent the reduction of ezrin and F-actin (green) at apical membrane after COM crystal treatment. Original magnification is 400X.

4. DISCUSSION AND CONCLUSION

The binding of COM crystals onto apical surface of renal tubular epithelial cells usually mediates by the interaction between crystal and microvilli of renal epithelial cells (23). This attachment of COM crystals can cause various cellular responses inside renal tubular epithelial cells including the production of reactive oxygen species (ROS), stimulation of various signaling molecules, destruction and transformation of microvilli and other intracellular organelles (4-6, 21). Microvilli breakdown, transformation and decreasing of their density on apical surface of renal tubular cells were also detected in the crystal-forming area by transmission electron microscopy (24) observation in glyoxylate-treated mouse kidneys at the early stage of glyoxylate administration (6 h) (4, 25). The number and length of microvilli in the glyoxylate-administrated mice were significantly reduced and they were fallen into the renal lumen during 24 h of glyoxylate administration (6, 25). Moreover, these findings implicated the involvement of microvillar injuries and the development of kidney stone disease *in vivo* (1, 21, 22). Notwithstanding these observations, the molecular basis focusing on microvilli disruption induced by COM crystal adhesion is still unknown.

This study, we aimed to investigate the molecular mechanism of microvillar injury in distal renal tubular epithelial (MDCK) cells which was occurred after COM crystal adhesion. Evidences of injured-microvilli lesion, apical F-actin staining was decreased the signal intensity referring to the reduction of microvillar density at apical surface of COM crystal-treated MDCK cells. Microvilli covering the apical surface of renal epithelial cells consist of a major core bundle of filamentous actin (F-actin) cytoskeleton and ezrin which acts as a cytoskeleton liker protein to connect membrane proteins with actin cytoskeleton and responsible for stabilizing microvilli of renal tubular epithelial cells (26, 27). We found the reduction of ezrin level in whole cell lysate extracted from COM crystal-treated cells with a statistically significant different in comparison with control group. This result is consistent with our previous studies which revealed the involvement of ezrin in response to COM crystal treatment in term of the alteration in protein level from 2D-PAGE data (11, 12). Further investigations were done by determining ezrin localization and distribution after COM crystal exposure in MDCK cells. Confocal images showed the interesting data which clearly revealed the reduction of ezrin at apical surface and the redistribution of ezrin from apical to basolateral while its protein level was decreased after COM crystal-treated cells. The similar result of redistribution was found in F-actin cytoskeleton while the protein level of β-actin was not changed after COM crystal treatment. These striking results of the decrease in ezrin level and its apical localization together with loss of apical F-actin

indicated the possible molecular mechanism leading to microvillar injury in response to COM crystal adhesion.

We next investigated whether COM crystal could induce the dissociation of ezrin from actin cytoskeleton by extracting control and COM crystal-treated cells with 0.5%Triton X-100-containing buffer. As expected, ezrin was selectively decreased in Triton X-100 insoluble fraction which represents cytoskeleton and cytoskeleton-associated proteins. This result indicated that ezrin was dissociated from the actin cytoskeleton after COM crystal treatment. Confocal images also showed the loss of apical ezrin and F-actin cytoskeleton in COM crystal-treated cells. Moreover, we observed the redistribution from apical to basolateral of ezrin and F-actin in the different serial focal planes of confocal data after incubation for 48 h with COM crystals. The posttranslational modification in term of threonine phosphorylation of ezrin was explored because the changes of phosphorylation state of ezrin can influence its functions. We found the increasing of ezrin in phosphothreonine protein pool which were isolated by performing immunoprecipitation with anti-phosphothreonine antibody. This data may be interpreted that ezrin was activated during COM crystal treatment by elevating threonine phosphorylation even its protein level was decreased. There are evidences demonstrating that the increase of phosphorylation level of ezrin can alter its cellular localization and pathological induce cell morphology changes (14, 28-30). Some signaling molecules which were stimulated in renal tubular cells in response to COM crystal adhesion could phosphorylate ezrin leading to the elevation of ezrin threonine phosphorylation (31-36). Further investigation needs to be done to explain the relation between ezrin phosphorylation and cellular pathogenesis in response to COM crystal exposure.

Redistribution of ezrin and actin cytoskeleton from apical structure to lateral surface at cell-cell contacts has been found in MDCK cells occurred under various physiological and pathological conditions (14, 37). These findings may represent an early stage of renal tubular cell injury leading to membrane protein polarity changes and dedifferentiation of renal tubular epithelial cells (37). Previous study suggested that the loss of ezrin level causes the destruction and decrease of microvilli both number and length (38). In addition, our present study reported that COM crystal treatment causes the dissociation of ezrin and actin cytoskeleton and could be correlated with microvillar disruption occurring during COM crystal adhesion. The adhesion of CaOx crystal onto renal tubular cells can trigger oxidative stress by increasing of reactive oxygen specie production which can cause extensive oxidative damage to cellular proteins (6, 21, 22). We detected the increasing of protein oxidation level by performing OxyBlot assay in COM crystal-treated cells in comparison with control group which was similar to previous researches (6, 21, 22). In general, oxidized proteins need to be degraded rapidly and effectively

by epithelial cells after encountering oxidative stress which may be catalyzed by proteasome function (39, 40).

Ezrin is documented that it is preferentially degraded under oxidative stress condition and its degradation may be the underlying mechanism leading to cell shape changes (41). From these reasons, it is possible that the reduction of ezrin level was caused by COM crystal-induced oxidative stress occurred in renal tubular epithelial cells. Moreover, the induction of oxidative stress can also play a critical role in the apical microvilli breakdown by reorganization of actin cytoskeleton (42, 43). Catechin which is one of the main components of green tea extract exerts as radical scavengers and can prevent COM crystallization and renal stone formation in rat (44, 45). Importantly, epigallocatechin-3-gallate (EGCG) is identified as a chemopreventive agent and has ability to inhibit proteasome function (46). Previous study showed that renal tubular epithelial cell injury and oxidative stress induced by calcium oxalate crystal were ameliorated by green tea administration in mice (6). Protein level and apical localization of ezrin were not reduced when we pretreated MDCK cells with green tea extract (EGCG) before exposure to COM crystals. There is possible that EGCG could act as antioxidant to prevent the induction of oxidative stress and reduce proteasome activity resulting in the stabilization of ezrin level and apical actin cytoskeleton during COM crystal treatment.

In conclusion, this study demonstrated that COM crystal treatment can induce the reduction and redistribution of ezrin and F-actin cytoskeleton in MDCK cells. The relation between ezrin and actin cytoskeleton was also decreased representing by Triton X-100 extraction assay. Oxidative stress is thought to be the major cause of ezrin degradation and actin cytoskeleton reorganization leading to apical microvillar breakdown and dysfunction. These alterations were prevented and reduced by the use of EGCG, an antioxidative chemical extracted from green tea. The data from this study could eventually contribute to understanding the molecular mechanism of microvillar injury in kidney stone patients and can be useful for future therapeutic benefits.

5. REFFERENCES

1. Tsujihata M. Mechanism of calcium oxalate renal stone formation and renal tubular cell injury. International journal of urology : official journal of the Japanese Urological Association. 2008;15(2):115-20.
2. Lieske JC, Deganello S. Nucleation, adhesion, and internalization of calcium-containing urinary crystals by renal cells. Journal of the American Society of Nephrology : JASN. 1999;10 Suppl 14:S422-9.
3. Lieske JC, Huang E, Toback FG. Regulation of renal epithelial cell affinity for calcium oxalate monohydrate crystals. American journal of physiology Renal physiology. 2000;278(1):F130-7.
4. Hirose M, Tozawa K, Okada A, Hamamoto S, Shimizu H, Kubota Y, et al. Glyoxylate induces renal tubular cell injury and microstructural changes in experimental mouse. Urol Res. 2008;36(3-4):139-47.
5. Khan SR, Hackett RL. The use of SEM in the study of oxalate induced experimental nephrolithiasis. Scanning electron microscopy. 1980(3):379-86.
6. Hirose M, Yasui T, Okada A, Hamamoto S, Shimizu H, Itoh Y, et al. Renal tubular epithelial cell injury and oxidative stress induce calcium oxalate crystal formation in mouse kidney. International journal of urology : official journal of the Japanese Urological Association. 2010;17(1):83-92.
7. Herzlinger DA, Easton TG, Ojakian GK. The MDCK epithelial cell line expresses a cell surface antigen of the kidney distal tubule. J Cell Biol. 1982;93(2):269-77.
8. Casaletto JB, Saotome I, Curto M, McClatchey AI. Ezrin-mediated apical integrity is required for intestinal homeostasis. Proceedings of the National Academy of Sciences of the United States of America. 2011;108(29):11924-9.
9. Bonventre JV, Yang L. Cellular pathophysiology of ischemic acute kidney injury. The Journal of clinical investigation. 2011;121(11):4210-21.
10. Sharfuddin AA, Molitoris BA. Pathophysiology of ischemic acute kidney injury. Nature reviews Nephrology. 2011;7(4):189-200.
11. Thongboonkerd V, Semangoen T, Sinchaikul S, Chen ST. Proteomic analysis of calcium oxalate monohydrate crystal-induced cytotoxicity in distal renal tubular cells. J Proteome Res. 2008;7(11):4689-700.
12. Semangoen T, Sinchaikul S, Chen ST, Thongboonkerd V. Proteomic analysis of altered proteins in distal renal tubular cells in response to calcium oxalate monohydrate crystal

adhesion: Implications for kidney stone disease. Proteomics Clinical applications. 2008;2(7-8):1099-109.

13. Chaiyarit S, Thongboonkerd V. Changes in mitochondrial proteome of renal tubular cells induced by calcium oxalate monohydrate crystal adhesion and internalization are related to mitochondrial dysfunction. J Proteome Res. 2012;11(6):3269-80.
14. Wu YX, Uezato T, Fujita M. Tyrosine phosphorylation and cellular redistribution of ezrin in MDCK cells treated with pervanadate. Journal of cellular biochemistry. 2000;79(2):311-21.
15. Chen J, Doctor RB, Mandel LJ. Cytoskeletal dissociation of ezrin during renal anoxia: role in microvillar injury. The American journal of physiology. 1994;267(3 Pt 1):C784-95.
16. Chen J, Cohn JA, Mandel LJ. Dephosphorylation of ezrin as an early event in renal microvillar breakdown and anoxic injury. Proceedings of the National Academy of Sciences of the United States of America. 1995;92(16):7495-9.
17. Fong-ngern K, Chiangjong W, Thongboonkerd V. Peeling as a novel, simple, and effective method for isolation of apical membrane from intact polarized epithelial cells. Anal Biochem. 2009;395(1):25-32.
18. Thongboonkerd V, Semangoen T, Chutipongtanate S. Factors determining types and morphologies of calcium oxalate crystals: molar concentrations, buffering, pH, stirring and temperature. Clin Chim Acta. 2006;367(1-2):120-31.
19. Bradford MM. A rapid and sensitive method for the quantitation of microgram quantities of protein utilizing the principle of protein-dye binding. Anal Biochem. 1976;72:248-54.
20. Blom N, Gammeltoft S, Brunak S. Sequence and structure-based prediction of eukaryotic protein phosphorylation sites. Journal of molecular biology. 1999;294(5):1351-62.
21. Davalos M, Konno S, Eshghi M, Choudhury M. Oxidative renal cell injury induced by calcium oxalate crystal and renoprotection with antioxidants: a possible role of oxidative stress in nephrolithiasis. Journal of endourology / Endourological Society. 2010;24(3):339-45.
22. Khan SR. Reactive oxygen species, inflammation and calcium oxalate nephrolithiasis. Translational andrology and urology. 2014;3(3):256-76.
23. Lieske JC, Swift H, Martin T, Patterson B, Toback FG. Renal epithelial cells rapidly bind and internalize calcium oxalate monohydrate crystals. Proceedings of the National Academy of Sciences of the United States of America. 1994;91(15):6987-91.

24. Lauffer BEL, Melero C, Temkin P, Lei C, Hong W, Kortemme T, et al. SNX27 mediates PDZ-directed sorting from endosomes to the plasma membrane. The Journal of Cell Biology. 2010;190(4):565-74.
25. Khan SR. Nephrocalcinosis in animal models with and without stones. Urol Res. 2010;38(6):429-38.
26. Brown JW, McKnight CJ. Molecular model of the microvillar cytoskeleton and organization of the brush border. PLoS One. 2010;5(2):e9406.
27. Zwaenepoel I, Naba A, Menezes Lyra Da Cunha M, Del Maestro L, Formstecher E, Louvard D, et al. Ezrin regulates microvillus morphogenesis by promoting distinct activities of Eps8 proteins. Molecular Biology of the Cell. 2012;23(6):1080-95.
28. Sarrió D, Rodríguez-Pinilla SM, Dotor A, Calero F, Hardisson D, Palacios J. Abnormal ezrin localization is associated with clinicopathological features in invasive breast carcinomas. Breast Cancer Research and Treatment. 2006;98(1):71-9.
29. Zhou R. Phosphorylation of ezrin on threonine 567 produces a change in secretory phenotype and repolarizes the gastric parietal cell. Journal of Cell Science. 2005;118(19):4381-91.
30. Viswanatha R, Ohouo PY, Smolka MB, Bretscher A. Local phosphocycling mediated by LOK/SLK restricts ezrin function to the apical aspect of epithelial cells. The Journal of Cell Biology. 2012;199(6):969-84.
31. Horuz R, Goktas C, Cetinel CA, Akca O, Aydin H, Ekici ID, et al. Role of TNF-associated cytokines in renal tubular cell apoptosis induced by hyperoxaluria. Urolithiasis. 2013;41(3):197-203.
32. Thamilselvan V, Menon M, Thamilselvan S. Selective Rac1 inhibition protects renal tubular epithelial cells from oxalate-induced NADPH oxidase-mediated oxidative cell injury. Urol Res. 2012;40(4):415-23.
33. Thamilselvan V, Menon M, Thamilselvan S. Oxalate-induced activation of PKC-alpha and -delta regulates NADPH oxidase-mediated oxidative injury in renal tubular epithelial cells. American journal of physiology Renal physiology. 2009;297(5):F1399-410.
34. Koul HK. Role of p38 MAP kinase signal transduction in apoptosis and survival of renal epithelial cells. Ann N Y Acad Sci. 2003;1010:62-5.
35. Koul HK, Menon M, Chaturvedi LS, Koul S, Sekhon A, Bhandari A, et al. COM crystals activate the p38 mitogen-activated protein kinase signal transduction pathway in renal epithelial cells. The Journal of biological chemistry. 2002;277(39):36845-52.

36. Gill DL, Mullaney JM, Ghosh TK. Intracellular calcium translocation: mechanism of activation by guanine nucleotides and inositol phosphates. The Journal of experimental biology. 1988;139:105-33.
37. Brown D, Lee R, Bonventre JV. Redistribution of villin to proximal tubule basolateral membranes after ischemia and reperfusion. The American journal of physiology. 1997;273(6 Pt 2):F1003-12.
38. Berryman M, Franck Z, Bretscher A. Ezrin is concentrated in the apical microvilli of a wide variety of epithelial cells whereas moesin is found primarily in endothelial cells. J Cell Sci. 1993;105 (Pt 4):1025-43.
39. Zhang YL, Cao YJ, Zhang X, Liu HH, Tong T, Xiao GD, et al. The autophagy-lysosome pathway: a novel mechanism involved in the processing of oxidized LDL in human vascular endothelial cells. Biochemical and biophysical research communications. 2010;394(2):377-82.
40. Xiong Y, Contento AL, Nguyen PQ, Bassham DC. Degradation of oxidized proteins by autophagy during oxidative stress in Arabidopsis. Plant Physiol. 2007;143(1):291-9.
41. Grune T, Reinheckel T, North JA, Li R, Bescos PB, Shringarpure R, et al. Ezrin turnover and cell shape changes catalyzed by proteasome in oxidatively stressed cells. FASEB journal : official publication of the Federation of American Societies for Experimental Biology. 2002;16(12):1602-10.
42. Huot J, Houle F, Marceau F, Landry J. Oxidative stress-induced actin reorganization mediated by the p38 mitogen-activated protein kinase/heat shock protein 27 pathway in vascular endothelial cells. Circ Res. 1997;80(3):383-92.
43. White P, Doctor RB, Dahl RH, Chen J. Coincident microvillar actin bundle disruption and perinuclear actin sequestration in anoxic proximal tubule. American journal of physiology Renal physiology. 2000;278(6):F886-93.
44. Kim H-S, Quon MJ, Kim J-a. New insights into the mechanisms of polyphenols beyond antioxidant properties; lessons from the green tea polyphenol, epigallocatechin 3-gallate. Redox Biology. 2014;2:187-95.
45. Zhai W, Zheng J, Yao X, Peng B, Liu M, Huang J, et al. Catechin prevents the calcium oxalate monohydrate induced renal calcium crystallization in NRK-52E cells and the ethylene glycol induced renal stone formation in rat. BMC complementary and alternative medicine. 2013;13:228.
46. Bonfili L, Cuccioloni M, Mozzicafreddo M, Cecarini V, Angeletti M, Eleuteri AM. Identification of an EGCG oxidation derivative with proteasome modulatory activity. Biochimie. 2011;93(5):931-40.

Output จากโครงการวิจัยที่ได้รับทุนจาก สกว.

1. ผลงานตีพิมพ์ในวารสารวิชาการนานาชาติ (ระบุชื่อผู้แต่ง ชื่อเรื่อง ชื่อวารสาร ปี เล่มที่ เลขที่ และหน้า)
   - Investigations of microvillar injury in renal tubular epithelial cells induced by calcium oxalate crystal adhesion
     (Manuscript in preparation)
2. การนำผลงานวิจัยไปใช้ประโยชน์
   - ผลการทดลองจากโครงการนี้มีประโยชน์อย่างมากในการอธิบายกลไกการบาดเจ็บของไมโครวิลไลที่ถูกเกาะจับโดยผลึกแคลเซี่ยมอ๊อกซาเลตโมโนไฮเดรต ซึ่งเป็นส่วนสำคัญในการทำหน้าที่ของเซลล์ท่อไต และยังเป็นการทดลองเบื้องต้นที่จะนำไปสู่การศึกษาวิจัยเชิงลึกในสัตว์ทดลองต่อไป นอกจากนี้ผลการทดลองที่ได้จะเป็นประโยชน์ในการคิดค้นการรักษาโรคนิ่วในไต เพื่อลดความรุนแรงและลดการเกิดโรคได้ในผู้ที่มีความเสี่ยงสูงเป็นต้น
3. อื่นๆ (เช่น หนังสือ การจดสิทธิบัตร)

ภาคผนวก

ประกอบด้วย Reprint หรือ Manuscript และบทความสำหรับการเผยแพร่

Investigations of microvillar injury in renal tubular epithelial cells induced by calcium oxalate crystal adhesion

Kedsarin Fong-ngern [1] *and Visith Thongboonkerd* [1, 2*]

[1]Medical Proteomics Unit, Office for Research and Development, Faculty of Medicine Siriraj Hospital, Mahidol University, Bangkok, Thailand

[2]Center for Research in Complex Systems Science, Mahidol University, Bangkok, Thailand

Running title: Microvillar injury after COM crystal exposure

Keyword: Kidney stone disease, Calcium oxalate, Microvillar injury, Renal tubular cell dysfunction

*Correspondence to:

Visith Thongboonkerd, MD, FRCPT

Medical Proteomics Unit, 6th Floor His Majesty The King 80th Birthday Anniversary 5th December 2007 Building, 2 Wanglang Road, Siriraj Hospital, Bangkoknoi, Bangkok 10700, Thailand

Phone/Fax: +66-2-4192850

E-mail: thongboonkerd@dr.com (or) vthongbo@yahoo.com

Abstract

The present study focused on the investigation of the pathogenic molecular mechanism during calcium oxalate monohydrate (COM) crystal exposure implicating in microvillar injury and disorganization in MDCK cells. Western blot analysis showed significantly reduced of ezrin level, which plays role in microvilli formation and stabilization in protein derived from COM crystal-treated cells. Laser scanning confocal microscopy revealed the decreases in F-actin staining pattern and ezrin localized at apical membrane of COM crystal-treated MDCK cells representing the reduction of their microvilli density. The reduction of apical localization of ezrin and actin cytoskeleton was further confirmed by apical membrane isolation and Western blotting. Using cytoskeletal extraction protocol by Triton X-100 detergent, cytoskeleton-associated ezrin level extracted from COM crystal-treated cells was significantly lower than control. OxyBlot analysis showed the increase in protein oxidation level in COM crystal-treated condition. The use of antioxidant chemical, EGCG (epigallocatechin-3-gallate), which extracted from green tea could reduce the level of protein oxidation and also prevented the reduction and stabilized apical localization of ezrin and actin cytoskeleton after COM crystal treatment. In conclusion, the present results demonstrated the reduction and apical membrane localization of ezrin and actin cytoskeleton which are core components of microvillar structure during COM crystal treatment. The induction of oxidative stress might be the cause and the use of EGCG could prevent these defects. These findings may provide the information as a platform to understand the pathogenesis leading to the loss of microvillar functions in kidney stone patients.

Abbreviations

CaOx	Calcium oxalate
COM	Calcium oxalate monohydrate
DNP	2,4-Dinitrophenol
DNPH	2,4-Dinitrophenylhydrazine
EDTA	Ethylenediaminetetraacetic acid
EGCG	Epigallocatechin-3-gallate
ERM	Ezrin, radixin, moesin
FBS	Fetal bovine serum
HRP	Horseradish peroxidase
MDCK	Madin-Darby canine kidney
MEM	Minimum essential medium
PBS	Phosphate buffer saline
ROS	Reactive oxygen species
SDS-PAGE	Sodium dodecyl sulfate polyacrylamide gel electrophoresis

Introduction

The binding of calcium oxalate monohydrate (COM) crystals onto apical surface of renal tubular epithelial cells usually mediates by the interaction between crystal and microvilli of renal epithelial cells (1). This attachment of COM crystal can cause various cellular responses triggering inside renal tubular epithelial cells including the production of reactive oxygen species (ROS), stimulation of signaling molecules, destruction and transformation of intracellular organelles (2-5). Microvilli breakdown, transformation and decreasing of their density on apical surface of renal tubular cells were also detected in the crystal-forming area by transmission electron microscopy (6) observation in glyoxylate-treated mouse kidneys at the early stage of glyoxylate administration (6 h) (2). The number and length of microvilli in the glyoxylated-administrated mice were significantly reduced and they were fallen in renal lumen during 24 h of glyoxylate administration (5, 7). Moreover, these findings implicated the involvement of microvillar injuries in the development of kidney stone disease (4, 8, 9).

Renal tubular epithelial cells are characterized as polarized cells, which plasma membrane is divided into apical and basolateral membranes to perform specialized transport functions (10). Apical surface is generally covered with numerous microvilli, which need some remarkable processes for their proper establishment and maintenance (11). The disruption and loss of microvilli density is the hallmark of renal tubular cell injury contributing to the development, severity, and kidney disease progression (12, 13). Microvillar injuries with evidences of blebbing, sloughing, internalization and decreasing their length and density can initiate renal tubular cell injuries and dysfunction in kidney stone patients (5, 8). Notwithstanding, the pathogenesis leading to microvillar injuries during COM crystal exposure in renal tubular cells has not been investigated.

In kidney stone disease, previous studies postulated and recognized the alteration of cellular structures and the disruption of microvillar organization both *in vivo* and *in vitro* models in response to oxalate and calcium oxalate (CaOx) crystal administrations (3, 5). Our

previous proteomics reports found that ezrin, which is one of ERM (ezrin, radixin, moesin) protein members and involves in the formation and maintenance of microvilli was changes its protein level in response to COM crystal adhesion (14-16). Ezrin acts as a linker between the cortical plasma membrane and actin cytoskeleton (11). The dissociation from actin cytoskeleton, the changes in distribution/localization and posttranslational modification in term of phosphorylation of ezrin can influence its functions (17-19).

Our interest was focused on the investigation of molecular mechanisms implicating in microvillar injuries in response to COM crystal exposure of MDCK cells. Western blotting and laser scanning confocal microscopy were performed to study the expression and localization of ezrin and actin cytoskeleton, which are the core components of apical microvilli in MDCK cells after exposure to COM crystals. Detergent solubility assay using Triton X-100 was used to determine actin cytoskeleton association of ezrin. Additionally, we also detected protein oxidation level with OxyBlot analysis and used epigallocatechin-3-gallate (EGCG), green tea extract to protect the cells from oxidative stress and determined its role in stabilizing ezrin and actin cytoskeleton localization after COM crystal treatment.

Materials and Methods

Antibodies and reagents

Mouse monoclonal anti-ezrin (4A5), anti-β-actin (C4) and anti-GAPDH (0411) were purchased from Santa Cruz biotechnology (Santa Cruz, CA, USA). Polyclonal HRP-conjugated secondary antibodies were obtained by DAKO Corporation (Hamburg, Germany). OxyBlot™ Protein Oxidation Detection Kit was provided from Chemicon International (Temecula, CA, USA). Oregon Green®488-conjugated phalloidin was available from Invitrogen Corporation (Grand Island, NY). Alexa Flour®488-conjugated and Alexa Flour®555-conjugated secondary antibodies were also purchased from Invitrogen. Hoechst 33342 was obtained by Molecular Probes (Burlington, Ontario, Canada). Epigallocatechin-3-gallate (EGCG) was provided by Sigma-Aldrich (St Louis, MO, USA).

Cell culture and COM crystal treatment

Mardin-Darby Canine kidney (MDCK) cells were grown in Eagle's minimum essential medium (MEM) (Gibco; Grand Island, NY) supplemented with 10%heat-inactivated fetal bovine serum (FBS) (Gibco), 1.2%penicillinG/streptomycin (Sigma, St.Louis, MO) and 2 mM of L-glutamine. The cells were maintained in a humidified incubator at 37°C with 5%CO_2 for 24 h. COM crystals (100 μg/ml) were prepared as described in previous study and resuspended in complete growth medium (20). Crystal suspension was added to 80%confluence MDCK cells and further incubated for 48 h in CO_2 incubator.

To obtain polarized MDCK monolayer, polycarbonate Transwell inserts (0.4 μm pore size; Corning Costar, Cambridge, MA, USA) were used as culture substrate. MDCK cells at a density of 7.5 X 10^4 cells/ml were split and grown on collagen type IV-coated polycarbonate membrane inserts overnight before COM crystal addition. The collagen type IV-coated polycarbonate membrane was prepared by adding of collagen type IV (6 μg/cm2) (Sigma, St. Louis, MO, USA) solution onto Transwell inserts by covering whole surface area and incubated at 4°C overnight.

Protein extraction and Western blotting

Control and COM crystal-treated cells were extracted in 1XLaemmli's buffer containing 60 mM Tris-HCl pH 6.8, 2%SDS, 10%glycerol, 5%β-mercaptoethanol and 0.01%bromophenol blue to obtain whole cell lysate. Protein concentration was measured and calculated according to Bradford's protein assay protocol (21). Cell lysates were resolved by 12%SDS-PAGE and then transferred onto nitrocellulose membrane (Millipore Corporation; Bedford, MA, USA). After blocking non-specific binding with 5%skim milk for 1 h, the nitrocellulose membranes were incubated with primary antibody for overnight at 4°C and corresponding secondary antibody for 1 h at room temperature, respectively. After washing with PBS, the immunoreactive band was detected by SuperSignal West Pico chemiluminescence substrate (Pierce Biotechnology, Inc., Rockford, IL) and exposed to X-ray film. Band signal intensity was measured by ImageMaster 2D Platinum 5.0 software (GE Healthcare, Waukesha, WI, USA).

Immunofluorescence and laser scanning confocal microscopy

Cells were cultured on glass slides or Transwell inserts for polarized MDCK cells. Cell morphology was firstly observed under a phase contrast microscope (Olympus CKX41; Tokyo, Japan) after COM crystal treatment for 48 h. For immunofluorescence staining, MDCK cells were washed twice with cold PBS containing 1mM $MgCl_2$ and 0.1 mM $CaCl_2$ or PBS^+. The cells were fixed with 4% paraformaldehyde and permeabilized with 0.1% Triton X-100 in PBS for 15 min at room temperature. After washing, primary antibody and corresponding secondary antibody were sequentially incubated for 1 h at 37°C, respectively. Stained cells were mounted in 50% glycerol/PBS on glass slice. The XY, XZ and YZ sections of these cells were acquired by using a Nikon A1R laser scanning confocal microscope (Nikon Instruments, Inc., New York, United States). The fluorescently stained cells were processed using NIS-Elements software (Nikon Corporation).

Apical membrane isolation by peeling method

MDCK monolayers were rinsed twice with ice-cold PBS^{+} (special containing 1 mM $MgCl_2$ and 0.1 mM $CaCl_2$) and then the solution was extremely aspirated (22). Whatman filter paper (Whatman®, Whatman International Ltd., Maidstone, England) was used to isolate the apical membrane of cell monolayers. Filter paper was pre-wetted in deionized water and then placed onto cell monolayer to cover the whole surface area of the cells. After 5 min of incubation, the filter paper was quickly removed, soaked in deionized water and then apical membrane suspension was concentrated by lyophilization. The isolated apical membrane powder was kept at -20°C for long term storage.

Triton X-100 solubility assay

To examine the effect of COM crystal treatment on the association of ezrin with actin cytoskeleton, Triton X-100 solubility assay and Western blot analysis were applied. Cell monolayers or the remaining part of monolayers after apical membrane peeling were washed three times with PBS and then the solution was extensively removed. Ice -cold Triton extraction buffer containing 0.5%Triton X-100, 10 mM Tris-HCl, pH 7.4, 100 mM NaCl, 300 mM sucrose and 2 mM EDTA was added to the cells and incubated for 15 min on ice. Thereafter, the extracted cells were centrifuged at 10,000 rpm for 15 min at 4°C. The supernatant was collected as the non-cytoskeleton and cytosolic protein (Triton-soluble) and the pellet was reserved as the cytoskeleton and cytoskeleton-associated protein (Triton-insoluble) fractions. The Triton-soluble fraction was then aspirated and precipitated by adding absolute ethanol to give a final concentration of 75%. Finally, both fractions were solubilized using 1X Laemmli's buffer to obtain protein solution for SDS-PAGE and Western blotting.

Epigallocatechin-3-gallate (EGCG) pretreatment and protein oxidation determination

EGCG was used as an antioxidant chemical to reduce level of protein oxidation in MDCK cells after COM crystal treatment. MDCK cells were seeded and grown overnight in CO_2 incubator to obtain 80% confluent monolayer. Growth medium was removed and then

the cells were incubated with 25 µM of EGCG for 30 min. Thereafter, COM crystals (100 µg/ml) were added to the cells and treated for 48 h in CO_2 incubator at 37°C.

Determination of protein oxidation level was performed using the manufacturer's guideline from OxyBlot™ Protein Oxidation Detection Kit protocol (Chemicon, Inc., Temecula, CA). First, an equal amount of protein from control and COM crystal-treated cell lysates was subjected to derivatization carbonyl groups which are represented the oxidative damage to a protein by a 2, 4-dinitrophenyl-hydrazone (DNP) moiety. Next, these derivatized proteins were resolved on 12%SDS-PAGE gel and then blotted onto nitrocellulose membranes. The membrane was block non-specific binding with 5%BSA in PBS for 30 min and then incubated with rabbit anti-DNPH antibody to detect the oxidative modified proteins. After washing, the membrane was further exposed to corresponding HRP-conjugated secondary antibody. Finally, membrane was washed twice in washing buffer (PBS containing 0.2%Tween-20). Protein bands were visualized by using SuperSignal West Pico chemiluminescence substrate and then exposed to X-ray film. Band signal intensity was measured by ImageMaster 2D Platinum 5.0 software (GE Healthcare).

Statistical analysis

The data was shown as mean ± SEM. Comparisons among groups were analyzed by unpaired Student's t test and one-way analysis of variance (ANOVA) with Tukey's posthoc test (SPSS; version 13.0). *P*-values less than 0.05 were considered statistically significant.

Results

The decrease of microvillar density of MDCK cells after exposure to COM crystals

To demonstrate the effect of COM crystal on apical microvillar density, we cultured MDCK cells in the absence (control) or presence (COM) of COM crystals for 48 h. Under phase contrast microscope, COM crystal-treated cells showed striking morphological changes including the highly irregular shape and poorly intact of cell monolayer (data not shown). It is well known that apical microvilli consist of a core of bundled actin filaments and consistent with the apical F-actin staining pattern. We next stained the cells with Oregon Green®488-conjugated phalloidin to see F-actin staining pattern, which reflects to microvilli density after COM crystal treatment. There is evidence of the decrease of microvillar structure at apical membrane of COM crystal-treated cells by exhibiting the lower apical F-actin signal and the loss of its normal staining pattern compared to control group (**Supplement 1A** and **1B**). The data suggested the decrease of apical microvillar density in MDCK cells after COM crystal treatment.

The decrease in the expression level of ezrin in MDCK cells after exposure to COM crystals

Microvillar structure generally compose of a core bundle of filamentous actin (F-actin) and ezrin, an actin-binding structural component, which are the main structural proteins influence the establishment and maintenance of microvilli in epithelial cells (23). To evaluate the effect of COM crystals on the level of ezrin and β-actin expression, we prepared protein lysate extracted from control and COM crystal-treated cells to perform Western blot analysis. The results demonstrated that an approximately 82 kDa band of ezrin was obviously decreased with a statistically significant difference ($p < 0.01$) in lysate derived from COM crystal-treated cells in comparison to control (**Figure 1A** and **1B**). There was no significant difference in the expression level of β-actin between control and COM crystal-treated cell lysates (**Figure 1C** and **1D**). From these data, we found the effect of COM crystal treatment in

the reduction of ezrin expression level but did not affect the expression level of β-actin in MDCK cells.

The decrease of ezrin and actin cytoskeleton at the apical membrane of MDCK cells after exposure to COM crystals

To function in stabilization and maintenance of epithelial microvillar structure, ezrin and actin cytoskeleton have to be concentrated at the apical pole, which is the location of microvilli covering throughout apical cell surface. We further evaluated the impact of COM crystal treatment on the distribution and localization of ezrin and actin cytoskeleton in MDCK cells by using immunofluorescence staining and confocal microscopy. In control cells, we found that ezrin was highly concentrated at the apical membrane, whereas actin cytoskeleton (F-actin) was concentrated in both apical and lateral membranes of MDCK cells as shown in **Figure 2A** and **Figure 3A**, respectively. In sharp contrast, COM crystal-treated MDCK cells clearly showed a striking decrease of ezrin and actin cytoskeleton, which were localized at the apical membrane of the cell monolayer (**Figure 2A** and **Figure 3A**). To confirm the immunofluorescence data indicating a decrease in apical localization of ezrin and actin cytoskeleton, we then isolated apical membrane of control and COM crystal-treated monolayer by peeling method using filter paper. The isolated apical membrane from both conditions were solubilized in Laemmli's buffer and then an equal amount of apical membrane protein mixture derived from both conditions were processed by Western blotting in parallel with their cytosolic fraction (the remaining part of cell monolayer after apical membrane peeling). Western blot data also demonstrated the selective decrease only in apical membrane proteins isolated from COM crystal-treated cells of ezrin and β-actin (**Figure 2B** and **Figure 3B**) whereas ezrin expression in the cytosolic fraction, which were extracted from the remaining part of monolayer after peeling was not changed. The data indicated that COM crystal treatment affected apical membrane localization of ezrin and actin cytoskeleton by reducing their localization at microvillar position in MDCK cells.

The alteration in the relation with actin cytoskeleton of ezrin in MDCK cells after exposure to COM crystals

To perform a function as an actin cytoskeletal linker protein at microvillar structure, ezrin link with apical actin filament using a C-terminal F-actin binding segment and its N-terminal FERM domain is used to interact with other integral membrane proteins. We further investigate whether the exposure to COM crystals could alter the relation between ezrin and F-actin cytoskeleton in MDCK cells. Selective detergent extraction, which was commonly used to isolate cytoskeleton and cytoskeleton-associated proteins, was applied by incubating the cells with 0.5%Triton X-100-containing buffer. Triton-insoluble fraction composed of cytoskeleton and cytoskeletal-associated proteins, whereas Triton-soluble fraction composed of non-cytoskeleton and cytosolic proteins, respectively. The amount of ezrin associated with the Triton-insoluble cytoskeletal fraction was significantly decreased in COM crystal-treated condition supporting by the Western blot data in **Figure 4A** and **4B**.

Confocal images also demonstrated the loss of apical membrane localization of ezrin and actin cytoskeleton in COM crystal-treated MDCK cells which clearly showed in XZ-scanned sections in the confocal planes capturing the apical surface of epithelial cells (apical) (**Figure 5**). Likewise, the confocal data revealed the interesting observation, which we found the recruitment and concentration of the remaining ezrin and actin cytoskeleton to the lateral border at the site of cell-cell contact in COM crystal-treated cells (**Figure 5C** and **Supplement 2**). Because active or functional ezrin is normally associated with actin cytoskeleton and mainly present at apical membrane of epithelial cells, we next isolated apical membrane of control and COM crystal-treated cells and then extracted with 0.5%Triton X-100-containing buffer. Western blot data showed a selective decreased of ezrin and actin cytoskeleton only in apical membrane which again implied the reduction of functional ezrin was observed after COM crystal treatment (**Figure 6**). From these, our data showed that COM crystal treatment in MDCK cells could reduce ezrin and actin cytoskeleton expression at the

apical membrane, which displays microvillar structure. Additionally, the association between ezrin and actin cytoskeleton was also disrupted. These alterations could drastically influence the integrity of microvilli structure of renal tubular epithelial cells during COM crystal exposure.

Protein oxidation level was increased in MDCK cells after exposure to COM crystals

Previous researches indicated the induction of oxidative stress can cause extensive oxidative damage to various cellular proteins in response to CaOx crystal adhesion of renal cells by the production of reactive oxygen species (5). This study, we determined whether the level of protein oxidation was increased in MDCK cells after COM crystal treatment by detecting the level of protein carbonylation, which is the end production of protein oxidation using OxyBlot assay. Protein oxidation may be the cause of ezrin degradation resulting in the decrease of its expression level after COM crystal treatment that was found in this study. The results showed that a statistically significant increase in protein carbonylation was found in protein lysate extracted from COM crystal-treated cells (**Figure 7A** and **7B**) indicating the induction of protein oxidation causes by COM crystal treatment. It is possible that COM crystal treatment could potentially induce cellular protein oxidation including ezrin leading to degradation and reduction of its expression level in MDCK cells. Moreover, oxidative stress condition could be the cause of the alteration of apical actin cytoskeleton resulting in the loss of microvillar structure.

Pretreatment with EGCG completely prevents the increase in protein oxidation and decrease of ezrin expression level in MDCK cells after exposure to COM crystals

From our data, we demonstrated the elevation of oxidized protein level in COM crystal-treated MDCK cells which could be the cause of ezrin degradation. Next, we used an antioxidant chemical, epigallocatechin galate (EGCG), which is extracted from green tea and has strong antioxidative activity to reduce the level of protein oxidation during COM crystal treatment. MDCK cells were pretreated with 25 μM of EGCG for 30 min before incubating

with 100 μg/ml of COM crystals for 48 h. We found the reduction of protein oxidation level in MDCK cells which were pretreated with EGCG as shown in **Figure 7A** and **7B**. As expected, EGCG pretreatment can protect MDCK cells from oxidative stress occurred during COM crystal treatment by significantly decrease the level of protein oxidation (**Figure 7A** and **7B**). In addition, the use of EGCG can also prevent the reduction of ezrin expression level during COM crystal treatment but did not affect the expression level of β-actin (**Figure 7C** and **7E**).

Pretreatment with EGCG partially protects the decrease in apical membrane localization of ezrin and actin cytoskeleton in MDCK cells after exposure to COM crystals

As our data show that pretreatment MDCK cells with EGCG can prevent the reduction of ezrin expression level by decreasing of protein oxidation during COM crystal treatment. We also used EGCG to pretreat the cells and then further examined its protective effect on the stabilization of apical membrane localization of ezrin and actin cytoskeleton during COM crystal treatment. EGCG pretreatment also showed a nearly complete protection of the loss of apical localization of ezrin and actin cytoskeleton in MDCK cells after COM crystal treatment observing under confocal microscope (**Figure 7F**). The results indicated that oxidative stress and the reduction in apical membrane localization of ezrin and actin cytoskeleton after COM crystal treatment and decreases were prevented by EGCG pretreatment. The use of EGCG could potentially be an effective therapeutic for kidney stone disease.

Discussion

The present study aimed to investigate the molecular mechanism of microvillar injury occurring in distal renal tubular epithelial (MDCK) cells after COM crystal treatment. Evidence of injured-microvilli lesion, apical actin cytoskeleton staining was decreased the signal intensity referring to the reduction of microvillar density at apical surface of COM crystal-treated MDCK cells. Microvilli covering the apical surface of epithelial cells consist of a major core bundle of filamentous actin (F-actin) cytoskeleton and ezrin which acts as a cytoskeletal liker protein to connect integral membrane proteins with actin cytoskeleton and responsible for stabilizing microvillar structure (24, 25). We found the reduction of ezrin expression level in whole cell lysate extracted from COM crystal-treated MDCK cells with a statistically significant different in comparison with control. This result is consistent with our previous studies which revealed the possible involvement of ezrin in response to COM crystal adhesion in term of the alteration in its expression level from 2D-PAGE data (14, 15). Further investigations were done by determining ezrin localization and distribution after COM crystal exposure in MDCK cells. Confocal images showed the interesting data which clearly revealed the redistribution of ezrin from apical to basolateral while its protein level was decreased after COM crystal treatment. The similar result was found in actin cytoskeleton while the protein level of β-actin was not changed. These striking results of the decrease in ezrin expression level and its apical membrane localization together with the loss of apical localization of actin cytoskeleton indicated the possible mechanism leading to microvillar injury in response to COM crystal adhesion.

We next investigated whether COM crystal could induce the dissociation of ezrin from actin cytoskeleton by extracting cytoskeletal fraction from control and COM crystal-treated MDCK cells with 0.5%Triton X-100-containing buffer. As expected, ezrin was selectively decreased in Triton X-100 insoluble fraction which represents cytoskeleton and cytoskeletal-associated proteins. This result indicated that ezrin was dissociated from the actin

cytoskeleton after COM crystal treatment. Confocal examination also showed the loss of apical ezrin and F-actin cytoskeleton in COM crystal-treated MDCK cells. Moreover, we observed the redistribution from apical to basolateral membrane of ezrin and F-actin in the different serial focal planes of confocal data in MDCK cells after incubation with COM crystals. Redistribution of ezrin and actin cytoskeleton from apical structure to lateral surface at the cell-cell contact sites has been found in MDCK cells occurred under various physiological and pathological conditions (17, 26). These findings may represent an early stage of renal tubular injury leading to membrane protein polarity changes and dedifferentiation of renal epithelial cells (26). Previous study suggested that the loss of ezrin level causes the destruction and decrease both number and length of epithelial microvilli (23). In addition, our present study reported that COM crystal treatment causes the dissociation of ezrin and actin cytoskeleton and could be correlated with microvillar disruption occurring during COM crystal adhesion. The adhesion of CaOx crystal onto renal tubular cells can induce oxidative stress by increasing the production of reactive oxygen species which can cause extensive oxidative damage to various cellular proteins (4, 5, 9). We detected the increasing of protein oxidation level by performing OxyBlot assay in COM crystal-treated cells compared to control and was supported by previous researches (4, 5, 9). In general, the oxidized proteins need to be degraded rapidly and effectively by epithelial cells after encountering oxidative stress which may be catalyzed by proteasome function (27, 28).

Ezrin is documented that it is preferentially degraded under oxidative stress condition and its degradation may be the underlying mechanism leading to epithelial cell shape changes under oxidative stress (29). From this reason, it is possible that the reduction of ezrin expression level is expected to be caused by COM crystal-induced oxidative stress occurred in renal tubular cells. Moreover, the induction of oxidative stress can also play a critical role in the apical microvillar breakdown by the reorganization of actin cytoskeleton, especially at the site of microvillar structure of renal epithelial cells (30, 31). Catechin which is one of the main

components of green tea extract exerts as radical scavengers and can prevent COM crystallization and renal stone formation in rat (32, 33). Importantly, epigallocatechin-3-gallate (EGCG) is identified as a chemopreventive agent and has ability to inhibit proteasome function (34). Previous study showed that renal tubular epithelial cell injury and oxidative stress, which were induced by CaOx crystal, were ameliorated by green tea administration in mice (5). In this study, we found that expression level and apical localization of ezrin were not reduced when we pretreated MDCK cells with EGCG before exposure to COM crystals. There is possible that EGCG could act as antioxidant to prevent the induction of oxidative stress and reduce proteasome activity resulting in the stabilization of ezrin level and apical membrane actin cytoskeleton during COM crystal treatment.

In conclusion, this study demonstrated that COM crystal treatment can induce the reduction and redistribution of ezrin and actin cytoskeleton in MDCK cells. The relation between ezrin and actin cytoskeleton was also decreased representing by Triton X-100 extraction assay. Oxidative stress is thought to be the major cause of ezrin degradation and actin cytoskeleton reorganization resulting in apical microvillar breakdown and dysfunction. These alterations were prevented and ameliorated by the use of EGCG, an antioxidative chemical extracted from green tea (**Figure 8**). The data from this study could eventually contribute to understanding the molecular mechanism of microvillar injury in kidney stone patients and can be useful for future therapeutic benefits.

Acknowledgement

This study was supported by The Thailand Research Fund (TRG5680008) and Mahidol University.

References

1. Lieske JC, Swift H, Martin T, Patterson B, Toback FG. Renal epithelial cells rapidly bind and internalize calcium oxalate monohydrate crystals. Proceedings of the National Academy of Sciences of the United States of America. 1994;91(15):6987-91.
2. Hirose M, Tozawa K, Okada A, Hamamoto S, Shimizu H, Kubota Y, et al. Glyoxylate induces renal tubular cell injury and microstructural changes in experimental mouse. Urol Res. 2008;36(3-4):139-47.
3. Khan SR, Hackett RL. The use of SEM in the study of oxalate induced experimental nephrolithiasis. Scanning electron microscopy. 1980(3):379-86.
4. Davalos M, Konno S, Eshghi M, Choudhury M. Oxidative renal cell injury induced by calcium oxalate crystal and renoprotection with antioxidants: a possible role of oxidative stress in nephrolithiasis. Journal of endourology / Endourological Society. 2010;24(3):339-45.
5. Hirose M, Yasui T, Okada A, Hamamoto S, Shimizu H, Itoh Y, et al. Renal tubular epithelial cell injury and oxidative stress induce calcium oxalate crystal formation in mouse kidney. International journal of urology : official journal of the Japanese Urological Association. 2010;17(1):83-92.
6. Lauffer BEL, Melero C, Temkin P, Lei C, Hong W, Kortemme T, et al. SNX27 mediates PDZ-directed sorting from endosomes to the plasma membrane. The Journal of Cell Biology. 2010;190(4):565-74.
7. Khan SR. Nephrocalcinosis in animal models with and without stones. Urol Res. 2010;38(6):429-38.
8. Tsujihata M. Mechanism of calcium oxalate renal stone formation and renal tubular cell injury. International journal of urology : official journal of the Japanese Urological Association. 2008;15(2):115-20.

9. Khan SR. Reactive oxygen species, inflammation and calcium oxalate nephrolithiasis. Translational andrology and urology. 2014;3(3):256-76.
10. Herzlinger DA, Easton TG, Ojakian GK. The MDCK epithelial cell line expresses a cell surface antigen of the kidney distal tubule. J Cell Biol. 1982;93(2):269-77.
11. Casaletto JB, Saotome I, Curto M, McClatchey AI. Ezrin-mediated apical integrity is required for intestinal homeostasis. Proceedings of the National Academy of Sciences of the United States of America. 2011;108(29):11924-9.
12. Bonventre JV, Yang L. Cellular pathophysiology of ischemic acute kidney injury. The Journal of clinical investigation. 2011;121(11):4210-21.
13. Sharfuddin AA, Molitoris BA. Pathophysiology of ischemic acute kidney injury. Nature reviews Nephrology. 2011;7(4):189-200.
14. Thongboonkerd V, Semangoen T, Sinchaikul S, Chen ST. Proteomic analysis of calcium oxalate monohydrate crystal-induced cytotoxicity in distal renal tubular cells. J Proteome Res. 2008;7(11):4689-700.
15. Semangoen T, Sinchaikul S, Chen ST, Thongboonkerd V. Proteomic analysis of altered proteins in distal renal tubular cells in response to calcium oxalate monohydrate crystal adhesion: Implications for kidney stone disease. Proteomics Clinical applications. 2008;2(7-8):1099-109.
16. Chaiyarit S, Thongboonkerd V. Changes in mitochondrial proteome of renal tubular cells induced by calcium oxalate monohydrate crystal adhesion and internalization are related to mitochondrial dysfunction. J Proteome Res. 2012;11(6):3269-80.
17. Wu YX, Uezato T, Fujita M. Tyrosine phosphorylation and cellular redistribution of ezrin in MDCK cells treated with pervanadate. Journal of cellular biochemistry. 2000;79(2):311-21.

18. Chen J, Doctor RB, Mandel LJ. Cytoskeletal dissociation of ezrin during renal anoxia: role in microvillar injury. The American journal of physiology. 1994;267(3 Pt 1):C784-95.

19. Chen J, Cohn JA, Mandel LJ. Dephosphorylation of ezrin as an early event in renal microvillar breakdown and anoxic injury. Proceedings of the National Academy of Sciences of the United States of America. 1995;92(16):7495-9.

20. Thongboonkerd V, Semangoen T, Chutipongtanate S. Factors determining types and morphologies of calcium oxalate crystals: molar concentrations, buffering, pH, stirring and temperature. Clin Chim Acta. 2006;367(1-2):120-31.

21. Bradford MM. A rapid and sensitive method for the quantitation of microgram quantities of protein utilizing the principle of protein-dye binding. Anal Biochem. 1976;72:248-54.

22. Fong-ngern K, Chiangjong W, Thongboonkerd V. Peeling as a novel, simple, and effective method for isolation of apical membrane from intact polarized epithelial cells. Anal Biochem. 2009;395(1):25-32.

23. Berryman M, Franck Z, Bretscher A. Ezrin is concentrated in the apical microvilli of a wide variety of epithelial cells whereas moesin is found primarily in endothelial cells. J Cell Sci. 1993;105 (Pt 4):1025-43.

24. Brown JW, McKnight CJ. Molecular model of the microvillar cytoskeleton and organization of the brush border. PLoS One. 2010;5(2):e9406.

25. Zwaenepoel I, Naba A, Menezes Lyra Da Cunha M, Del Maestro L, Formstecher E, Louvard D, et al. Ezrin regulates microvillus morphogenesis by promoting distinct activities of Eps8 proteins. Molecular Biology of the Cell. 2012;23(6):1080-95.

26. Brown D, Lee R, Bonventre JV. Redistribution of villin to proximal tubule basolateral membranes after ischemia and reperfusion. The American journal of physiology. 1997;273(6 Pt 2):F1003-12.

27. Zhang YL, Cao YJ, Zhang X, Liu HH, Tong T, Xiao GD, et al. The autophagy-lysosome pathway: a novel mechanism involved in the processing of oxidized LDL in human vascular endothelial cells. Biochemical and biophysical research communications. 2010;394(2):377-82.

28. Xiong Y, Contento AL, Nguyen PQ, Bassham DC. Degradation of oxidized proteins by autophagy during oxidative stress in Arabidopsis. Plant Physiol. 2007;143(1):291-9.

29. Grune T, Reinheckel T, North JA, Li R, Bescos PB, Shringarpure R, et al. Ezrin turnover and cell shape changes catalyzed by proteasome in oxidatively stressed cells. FASEB journal : official publication of the Federation of American Societies for Experimental Biology. 2002;16(12):1602-10.

30. Huot J, Houle F, Marceau F, Landry J. Oxidative stress-induced actin reorganization mediated by the p38 mitogen-activated protein kinase/heat shock protein 27 pathway in vascular endothelial cells. Circ Res. 1997;80(3):383-92.

31. White P, Doctor RB, Dahl RH, Chen J. Coincident microvillar actin bundle disruption and perinuclear actin sequestration in anoxic proximal tubule. American journal of physiology Renal physiology. 2000;278(6):F886-93.

32. Kim H-S, Quon MJ, Kim J-a. New insights into the mechanisms of polyphenols beyond antioxidant properties; lessons from the green tea polyphenol, epigallocatechin 3-gallate. Redox Biology. 2014;2:187-95.

33. Zhai W, Zheng J, Yao X, Peng B, Liu M, Huang J, et al. Catechin prevents the calcium oxalate monohydrate induced renal calcium crystallization in NRK-52E cells and the ethylene glycol induced renal stone formation in rat. BMC complementary and alternative medicine. 2013;13:228.

34. Bonfili L, Cuccioloni M, Mozzicafreddo M, Cecarini V, Angeletti M, Eleuteri AM. Identification of an EGCG oxidation derivative with proteasome modulatory activity. Biochimie. 2011;93(5):931-40.

Figure legends

Figure 1: Decreasing of ezrin level in MDCK cells after COM crystal treatment. MDCK cells were grown in the absence (Control) or presence of 100 µg/ml of COM crystals (COM) for 48 h. (A) Representative Western blotting of ezrin and GAPDH (loading control) levels in whole cell lysate extracted from control and COM crystal-treated MDCK cells. (B) Relative band intensity of ezrin was normalized to GAPDH for each individual and the data are presented as means ± SEM of 3 independent experiments. (* $P < 0.01$ compared to control)

Figure 2: Selective decrease of ezrin at apical membrane of MDCK cells after COM crystal treatment. MDCK cells were grown on polycarbonate membrane in Transwell in the absence (Control) or presence of COM crystals (COM) for 48 h. (A) Localization and distribution of ezrin in control and treated cells were observed under laser scanning confocal microscope. Ezrin was shown in red and nucleus was shown in blue. The confocal images were captured from both horizontal at the level of apical membrane (XY) and sagittal obtained from apical to basal (XZ) sections of the cells. Original magnification = 400X in all panels. Apical membranes of control and COM crystal-treated cells were peeled (Apical) and the remaining portions were extracted (Cytosolic). (B) Western blotting of ezrin in apical membrane and cytosolic fractions extracted from control and COM crystal-treated MDCK cells.

Figure 3: Selective decrease of actin cytoskeleton at apical membrane of MDCK cells after COM crystal treatment. MDCK cells were grown on polycarbonate membrane in Transwell in the absence (control) or presence of COM crystals (COM) for 48 h. (A) Distribution and organization of F-actin in control and treated cells were observed under laser scanning confocal microscope. F-actin was stained with Oregon Green®488-conjugated phalloidin and shown in green and nucleus was shown in blue. The confocal images were captured from both horizontal at the level of apical membrane (XY) and sagittal obtained from apical to basal

(XZ) sections of the cells. Original magnification = 400X in all panels. (B) Western blotting of β-actin in apical membrane and cytosolic fractions extracted from control and COM crystal-treated MDCK cells.

Figure 4: Triton solubility of ezrin in control and COM crystal-treated MDCK cells. (A) Western blot analysis of ezrin in Triton-insoluble (cytoskeleton and cytoskeleton-associated proteins) and Triton-soluble (non-cytoskeleton and cytosolic proteins) fractions extracted from control and COM crystal-treated cells. The cells were extracted in extraction buffer containing 0.5%Triton X-100 for 15 min at 4°C and Triton-insoluble and -soluble fractions were obtained by centrifugation. (B) Relative band intensity of ezrin in Triton-insoluble and Triton-soluble fractions extracted from control and COM crystal-treated MDCK cells. Data are presented as means ± SEM of 3 independent experiments. COM crystal exposure causes a significant decrease in cytoskeleton-associated ezrin (Triton-insoluble fraction). (* $P < 0.05$ compared to control)

Figure 5: Distribution and colocalization between ezrin and F-actin cytoskeleton in different serial focal planes from apical to basal of control (A) and COM crystal-treated (B) MDCK cells. MDCK cells were grown in the absence (Control) or presence (COM) of COM crystals for 48 h. Cells were fixed, permeabilized and subjected to stain with anti-ezrin antibody (red) and Oregon Green®488-conjugated phalloidin for F-actin staining (green). Fluorescence images were obtained by confocal microscopy. XY sections at the apical membrane (Apical), middle (Middle) and basal membrane (Basal) of control and COM crystal-treated cells were shown. XZ sections obtained from apical to basal of cell monolayers were shown in C. Original magnification = 400X in all panels.

Figure 6: MDCK cells were incubated in the absence (Control) or presence of COM crystals (COM) for 48 h. The cells were isolated apical membrane by peeling and the remaining portion of cell monolayers were extracted with extraction buffer containing 0.5%Triton X-100 to obtain Triton-insoluble and Triton-soluble fractions. Western blot analysis of ezrin (A) and β-actin (C) in the apical membrane, Triton X-100-insoluble and Triton X-100-soluble fractions were presented and band intensity of ezrin (B) and β-actin (D) were quantified and demonstrated as mean ± SEM of 3 independent experiments. (* $P < 0.05$ compared to control)

Figure 7: Protein oxidation levels in MDCK cells in the absence or presence of COM crystals with EGCG pretreatment using OxyBlot methodology. (A) Representative Western blot analysis of proteins extracted from control and COM crystal-treated MDCK cells in the absence or presence of 25 µM of EGCG pretreatment for 30 min. (B) Quantitative analyses from 3 separate blots were presented by normalization to condition and expressed as mean ± SEM. Western blot analysis of ezrin and β-actin in proteins which were extracted from cells treated with the similar conditions (C). Relative band intensities of ezrin and β-actin to GAPDH were quantified and presented as mean ± SEM of 3 independent experiments (D and E). Ezrin (red), F-actin cytoskeleton (green) distribution and cell morphology of control and COM crystal-treated MDCK cells with or without EGCG pretreatment were observed under confocal and phase contrast microscopes (F). XY section was captured at the apical membrane and XZ section was obtained from apical to basal of cell monolayers. Original magnification of phase contrast and confocal microscopes are 200X and 400X, respectively. (* $P < 0.05$ compared to control, ** $P < 0.05$ compared to COM and *** $P < 0.05$ compared to 25 µM EGCG)

Figure 8: Possible mechanism of microvillar injury induces by COM crystal exposure. (A) Renal tubular epithelial cells were attached by COM crystals leading to the induction of

oxidative stress (B). Protein oxidations and their degradation were increased resulting in the reduction of ezrin and breakdown of actin cytoskeleton (C). Decreasing of ezrin and oxidative stress-induced actin cytoskeleton disorganization could reduce their apical membrane localizations and initiated microvillar injury and disruption (D, E). The use of an antioxidant chemical, EGCG could protect renal tubular cells from the induction of oxidative stress during exposure to COM crystals and prevent the reduction of ezrin and F-actin at apical membrane (F).

Supplement 1: Microvilli which covering the apical surface of control and COM crystal-treated MDCK cells was visualized both XY (A) and XZ (B) sections by phalloidin-labeled F-actin using laser scanning confocal microscopy (scale bar = 10 μm).

Supplement 2: Serial confocal images of control and COM crystal-treated polarized MDCK cells with or without 25 μM of EGCG pretreatment from apical to basolateral membranes of cell monolayers. Confocal microscopy slices captured of ezrin (A), F-actin (B) and their colocalization (C) from the apical to basal membrane sections of MDCK cells. Nucleus was stained with Hoechst dye and shown in blue (D).

Figure 1

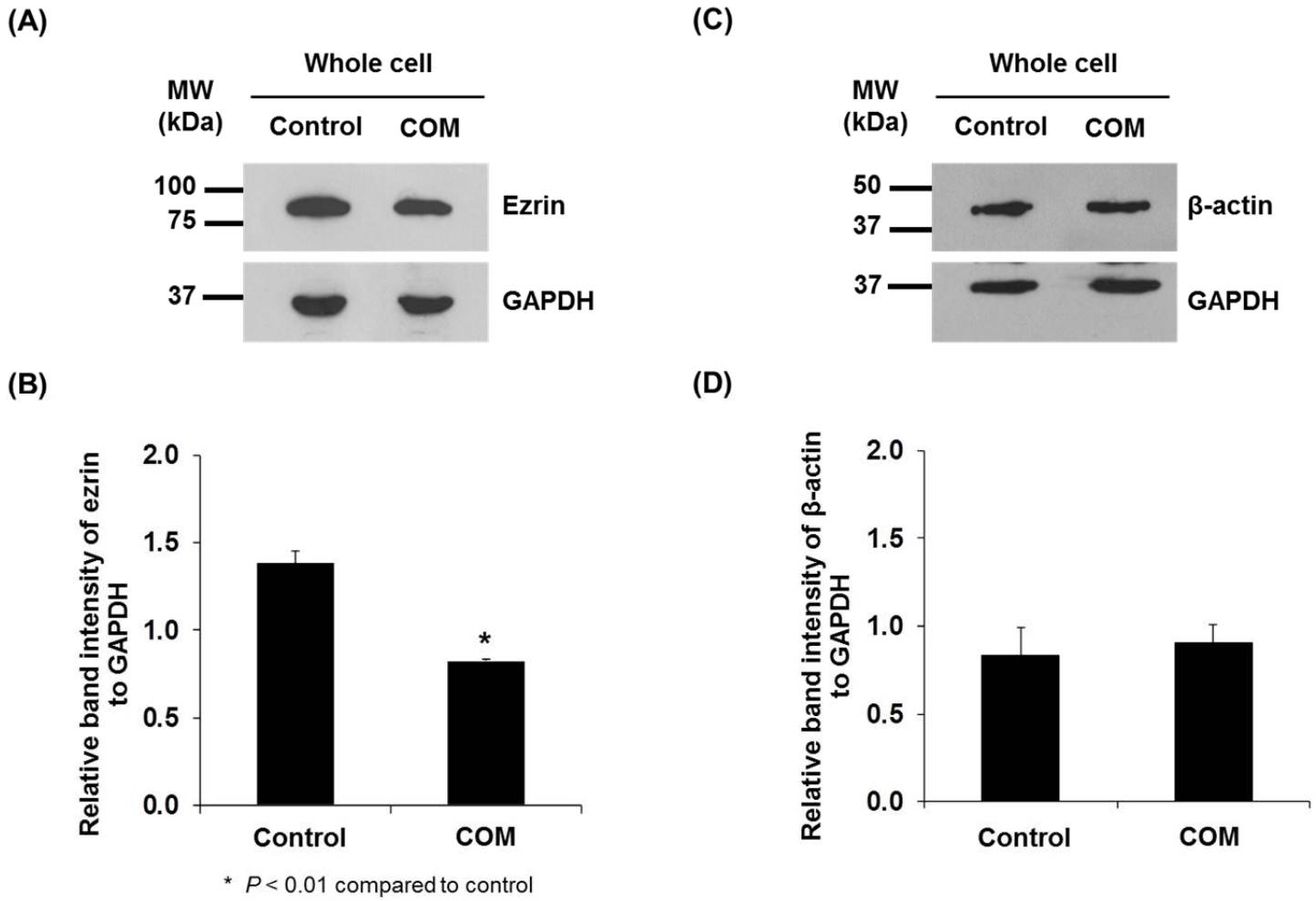
(A)
Whole cell
MW (kDa)
Control
COM
100
75
Ezrin
37
GAPDH
(C)
Whole cell
MW (kDa)
Control
COM
50
37
β-actin
37
GAPDH
(B)
Relative band intensity of ezrin to GAPDH
2.0
1.5
1.0
0.5
0.0
*
Control
COM
* P < 0.01 compared to control
(D)
Relative band intensity of β-actin to GAPDH
2.0
1.5
1.0
0.5
0.0
Control
COM

Figure 2

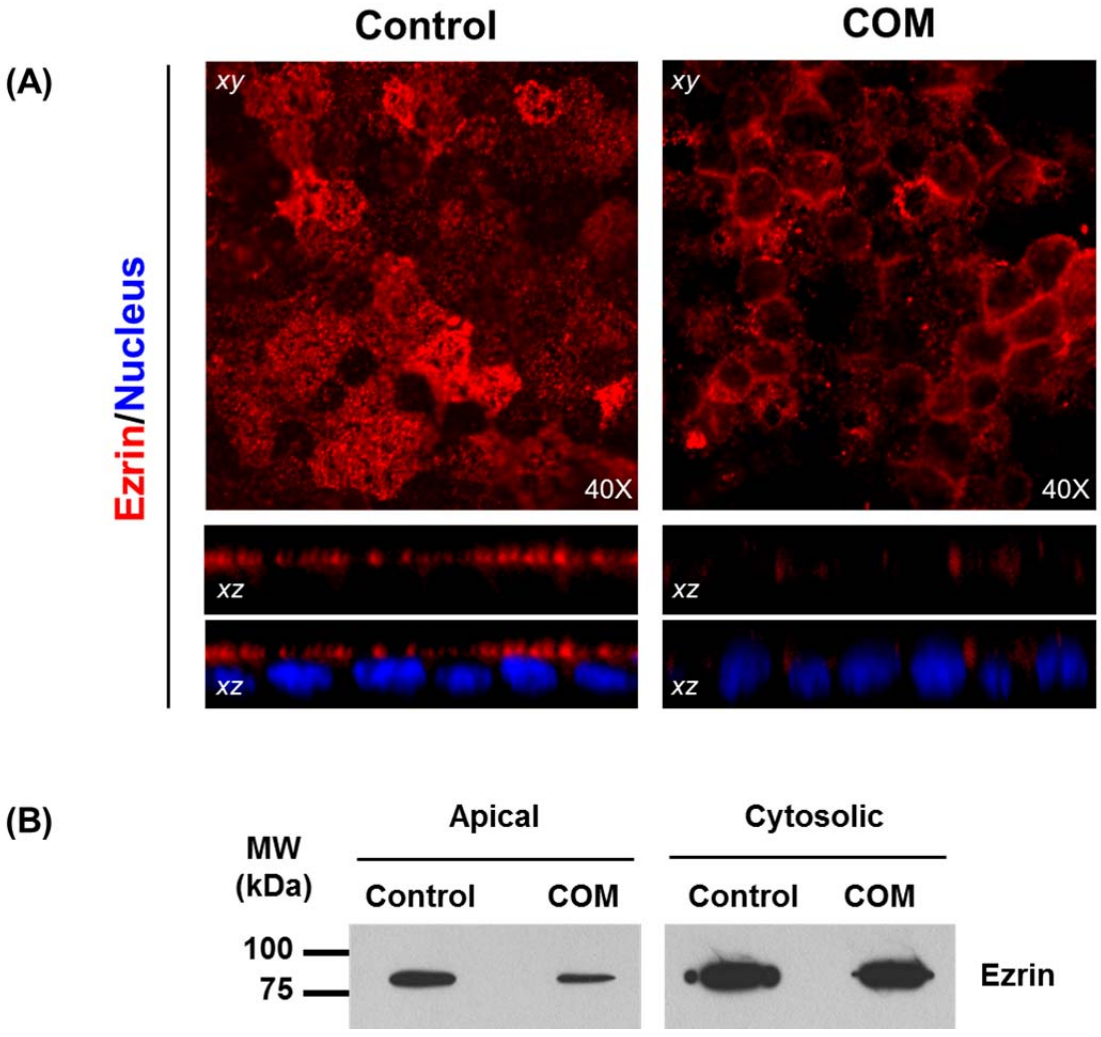
(A)
Control
COM
Ezrin/Nucleus
xy
40X
xz
(B)
Apical
Cytosolic
MW
(kDa)
Control
COM
Control
COM
100
75
Ezrin

Figure 3

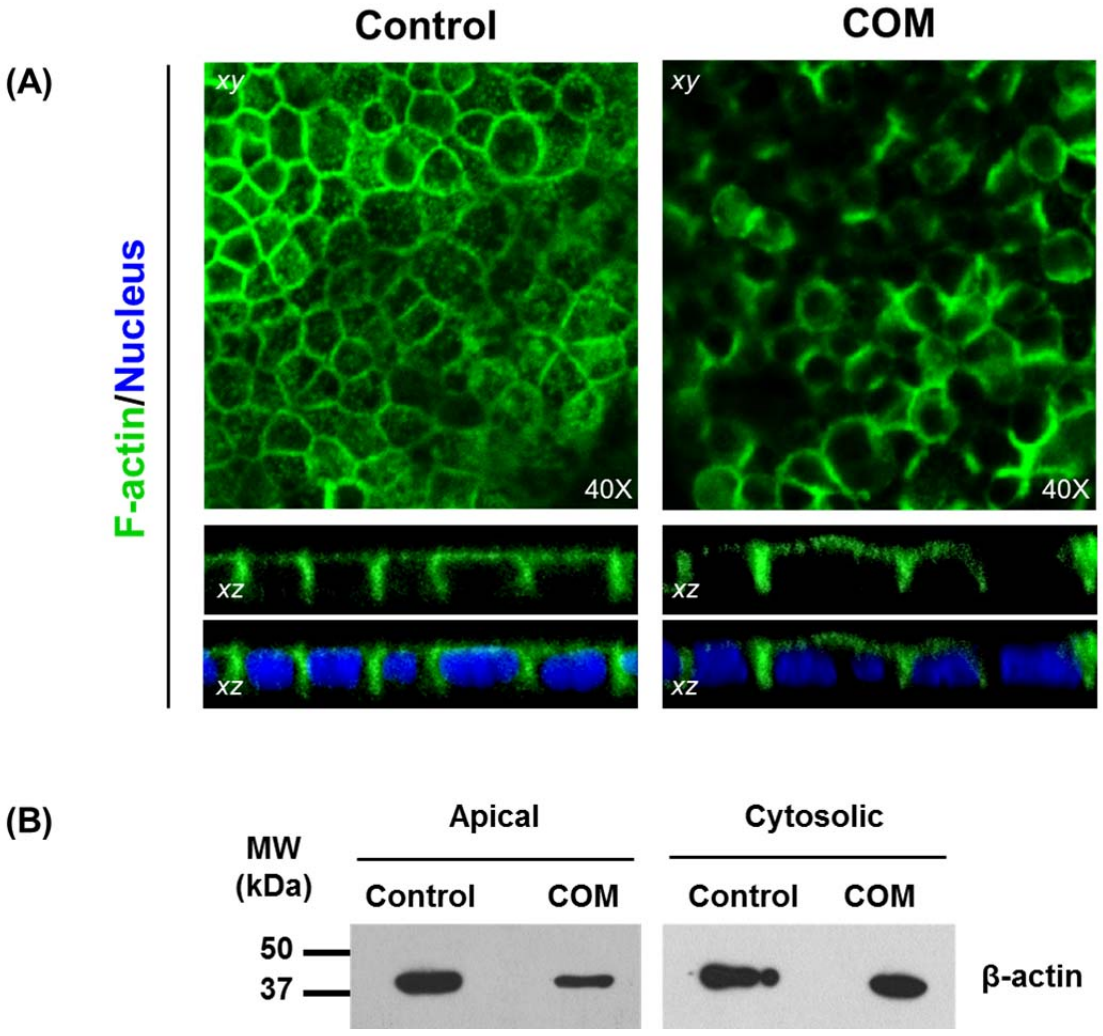
(A)
Control
COM
F-actin/Nucleus
xy
40X
xz
(B)
Apical
Cytosolic
MW
(kDa)
Control
COM
Control
COM
50
37
β-actin

Figure 4

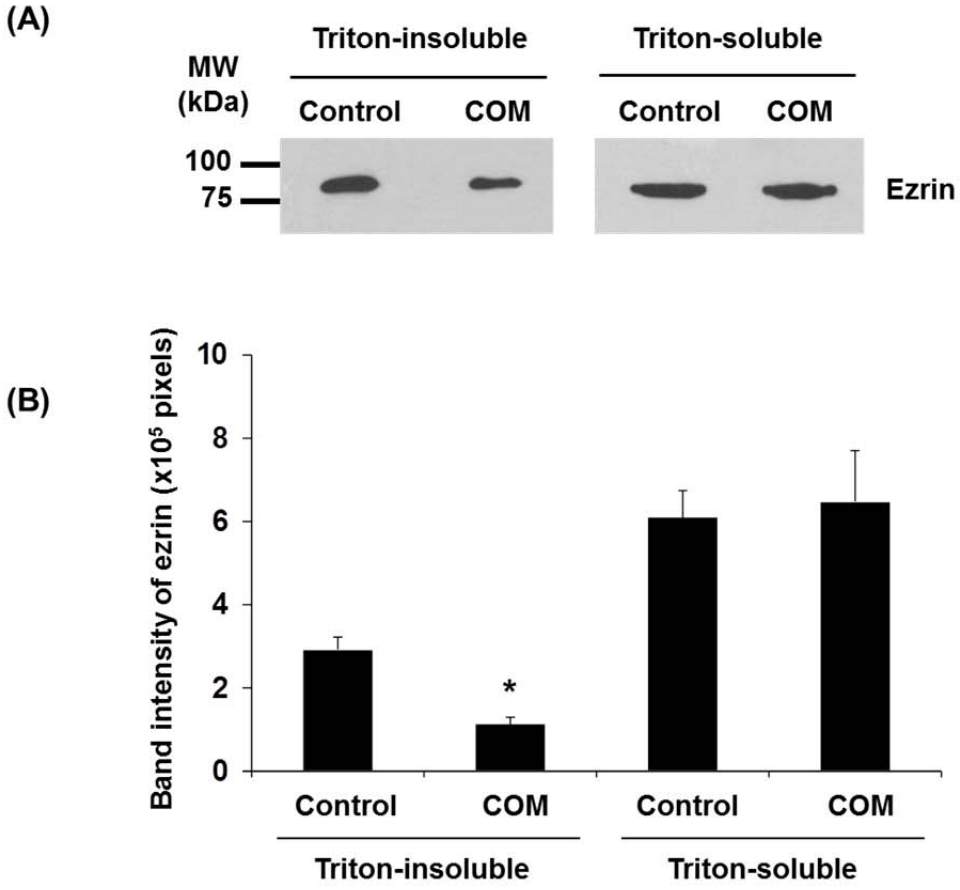

* $P < 0.05$ compared to control

Figure 5A

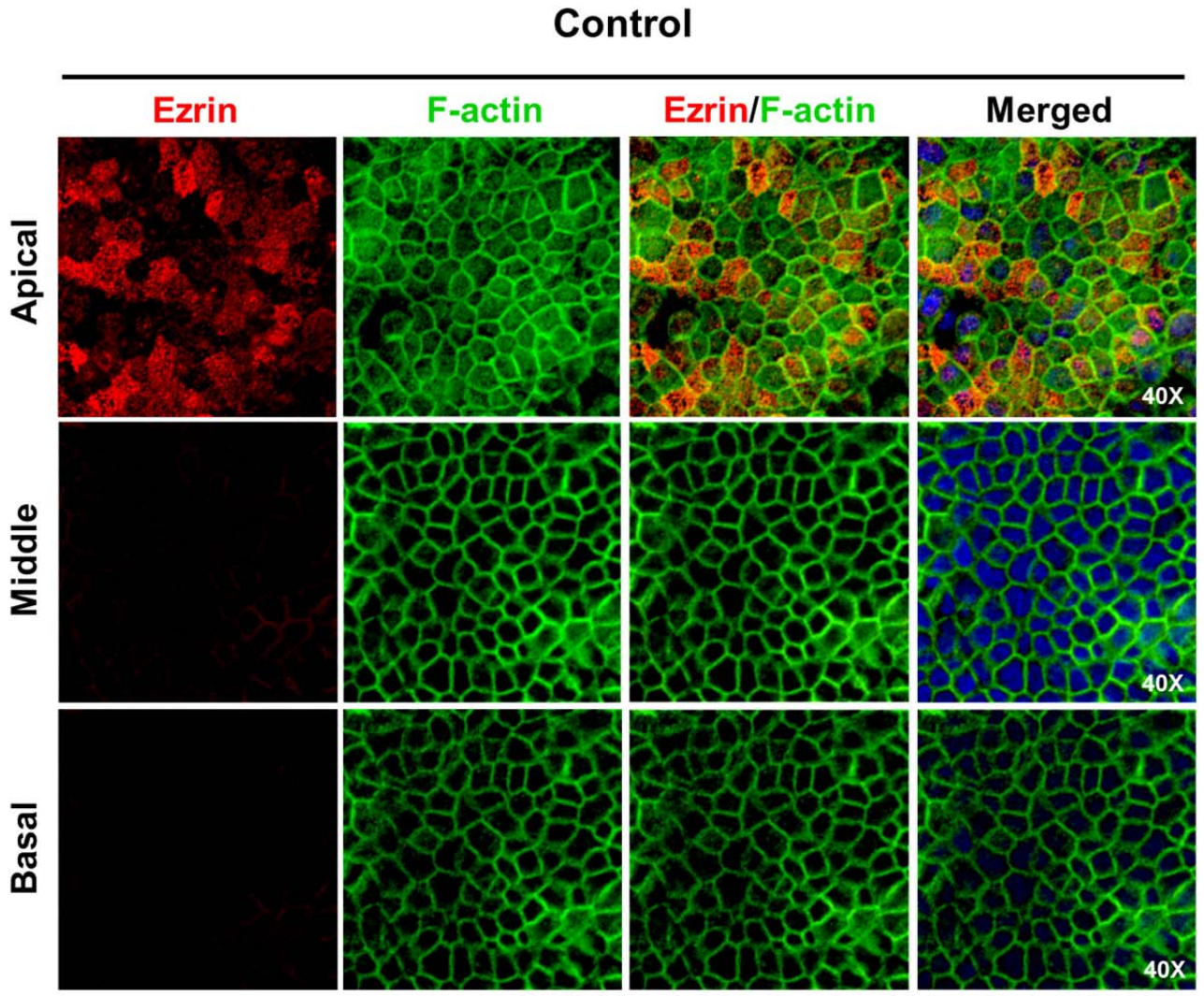
Control
Ezrin
F-actin
Ezrin/F-actin
Merged
Apical
Middle
Basal
40X
40X
40X

Figure 5B

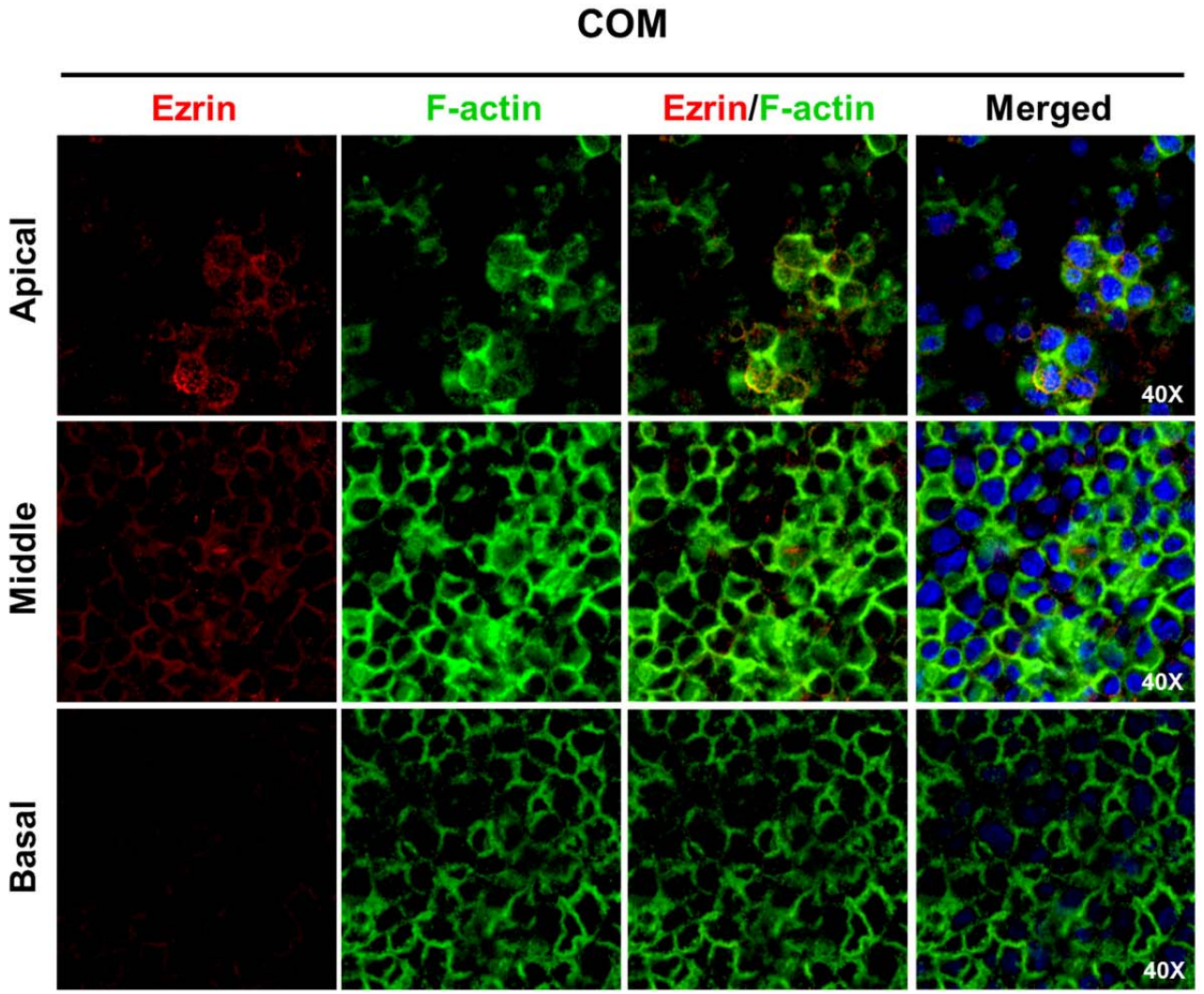
COM
Ezrin
F-actin
Ezrin/F-actin
Merged
Apical
Middle
Basal
40X
40X
40X

Figure 5C

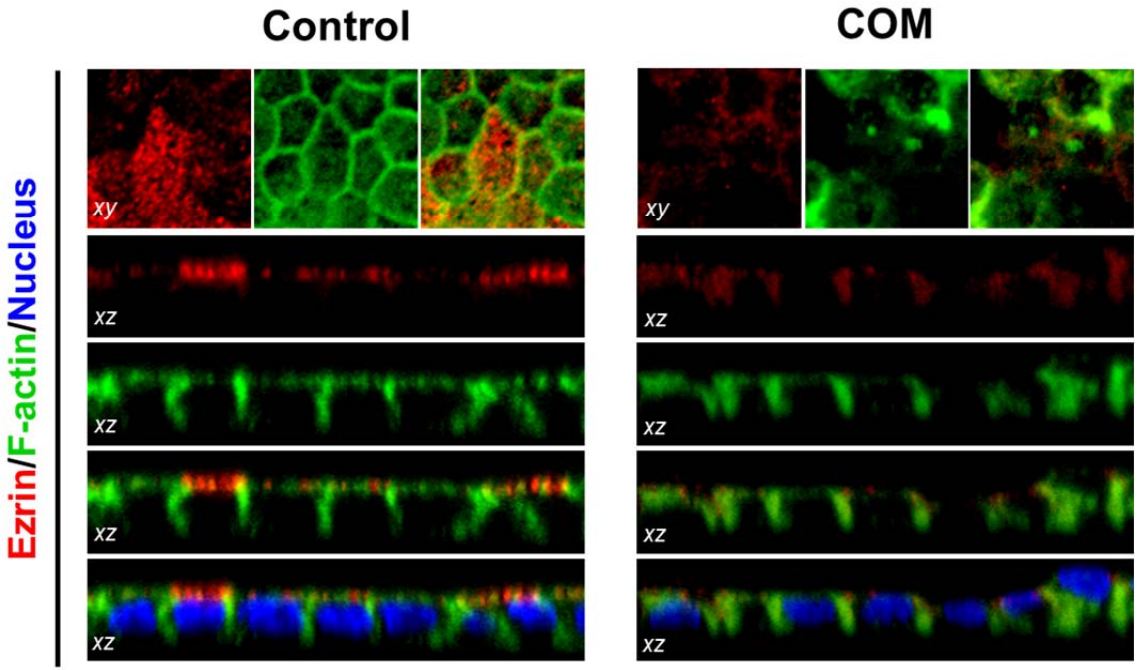

Figure 6

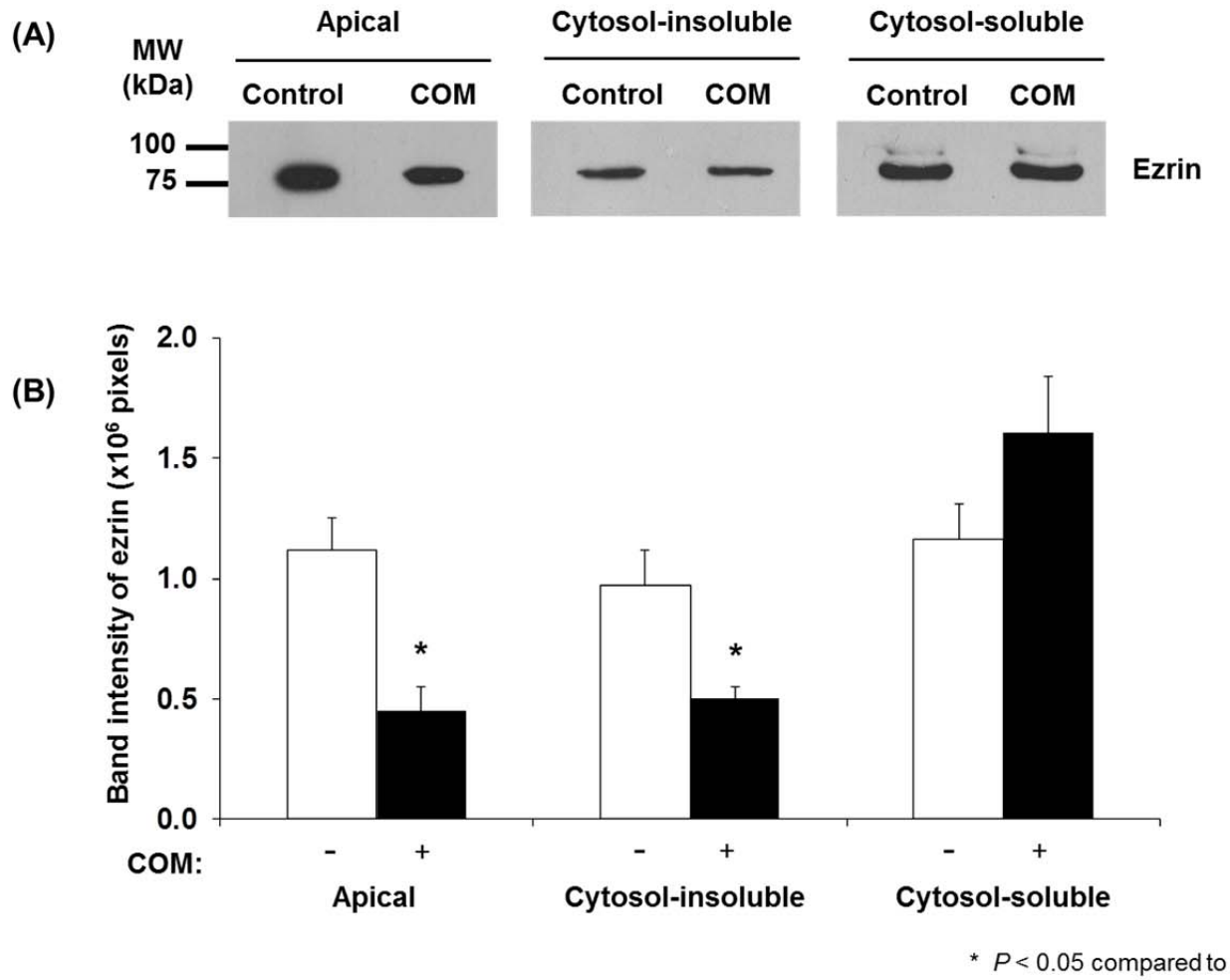

* $P < 0.05$ compared to control

Figure 6

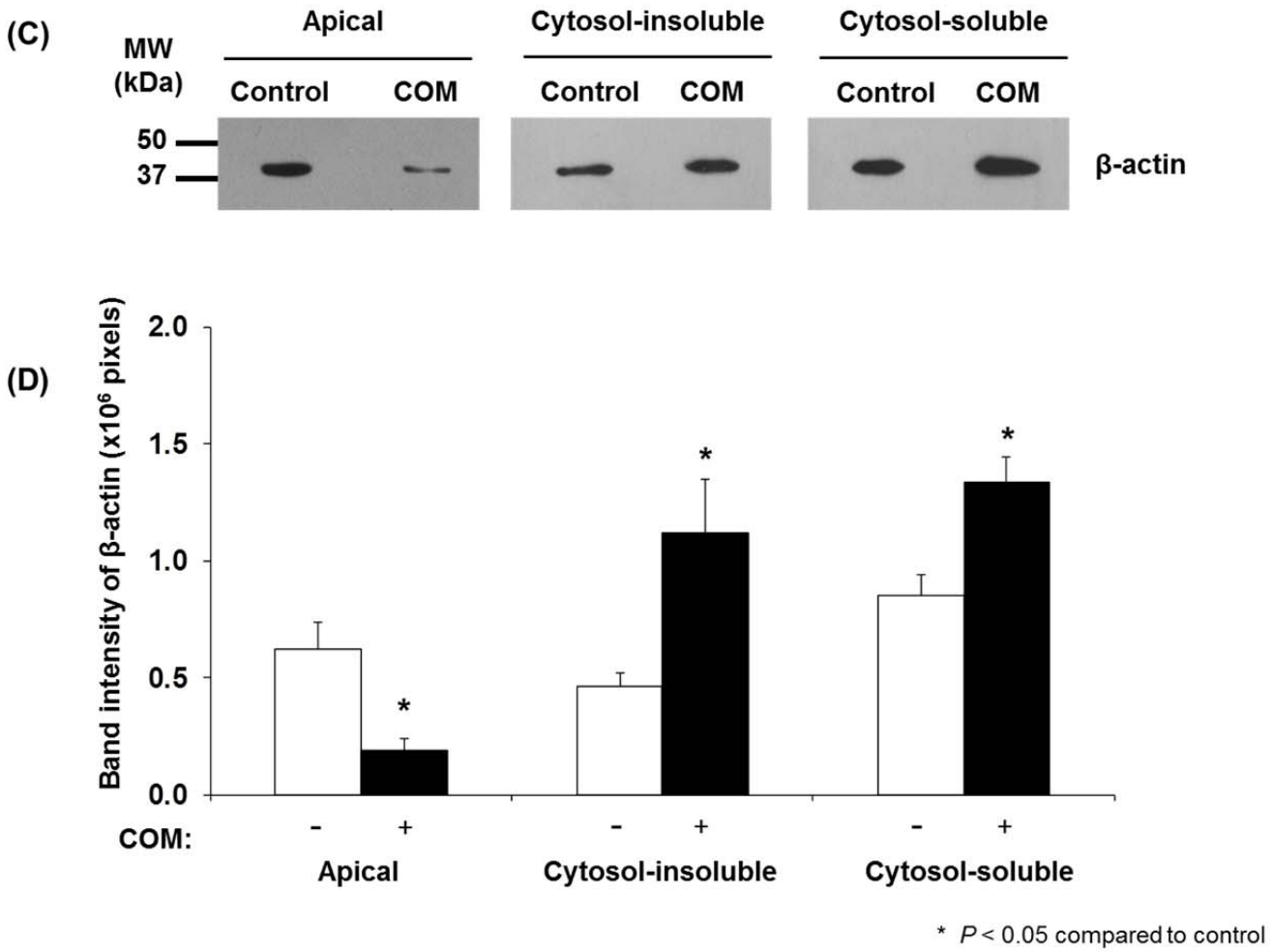

* $P < 0.05$ compared to control

Figure 7

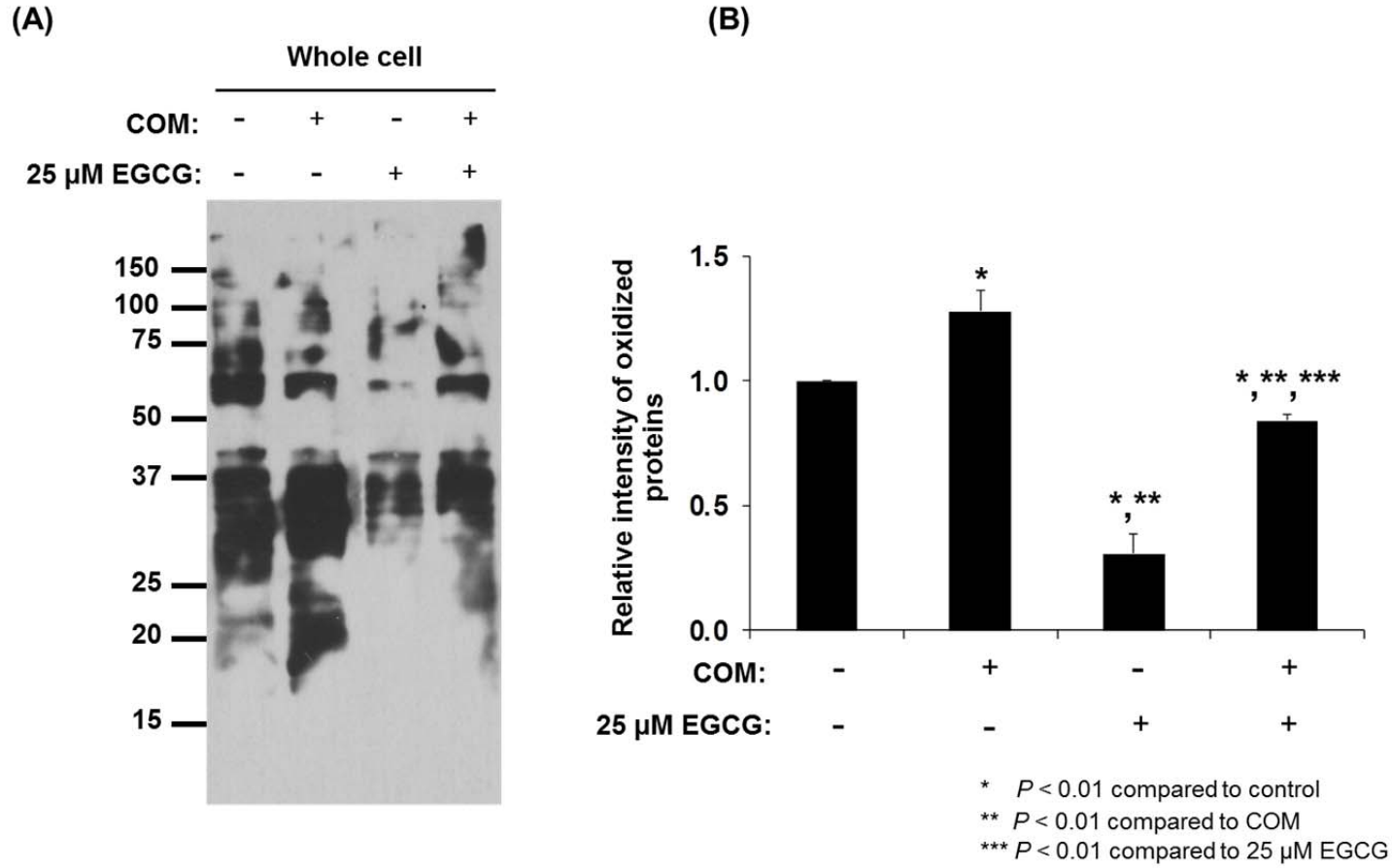
(A)
Whole cell
COM: - + - +
25 μM EGCG: - - + +
150
100
75
50
37
25
20
15
(B)
Relative intensity of oxidized proteins
1.5
1.0
0.5
0.0
*
*, **
*, **, ***
COM: - + - +
25 μM EGCG: - - + +
* P < 0.01 compared to control
** P < 0.01 compared to COM
*** P < 0.01 compared to 25 μM EGCG

Figure 7

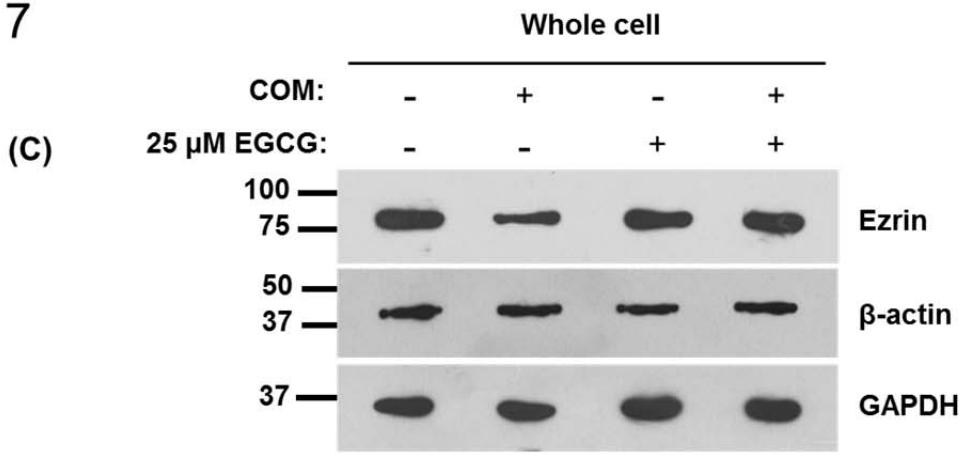
(C)
Whole cell
COM: - + - +
25 μM EGCG: - - + +
100
75
50
37
37
Ezrin
β-actin
GAPDH

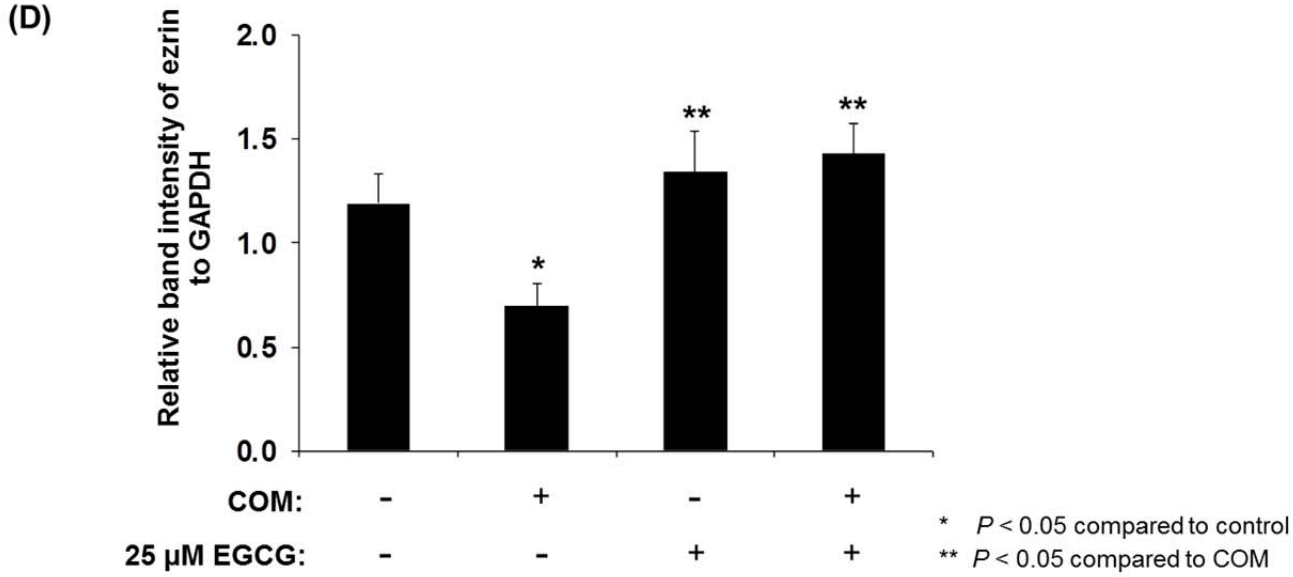
(D)
Relative band intensity of ezrin to GAPDH
2.0
1.5
1.0
0.5
0.0
*
**
**
COM: - + - +
25 μM EGCG: - - + +
* P < 0.05 compared to control
** P < 0.05 compared to COM

(E)

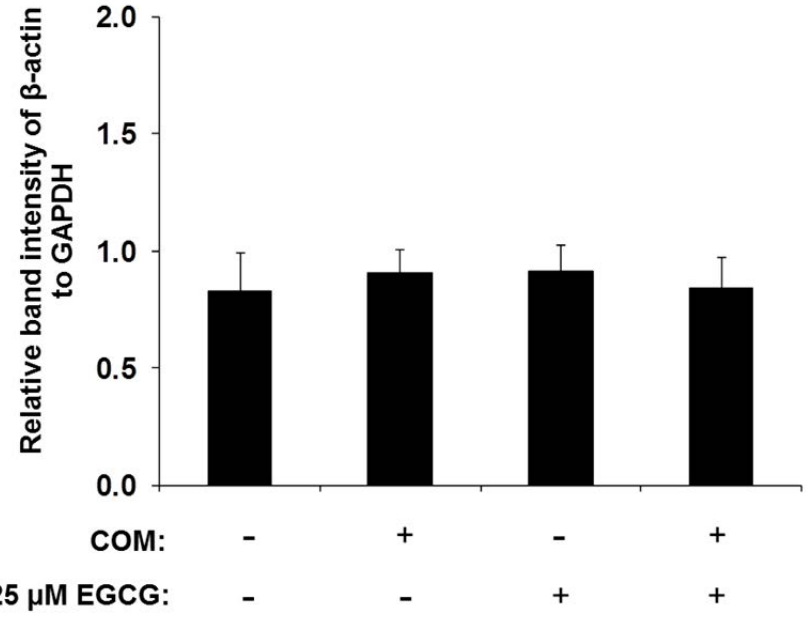
Relative band intensity of β-actin to GAPDH
2.0
1.5
1.0
0.5
0.0
COM:
-
+
-
+
25 μM EGCG:
-
-
+
+

(F)

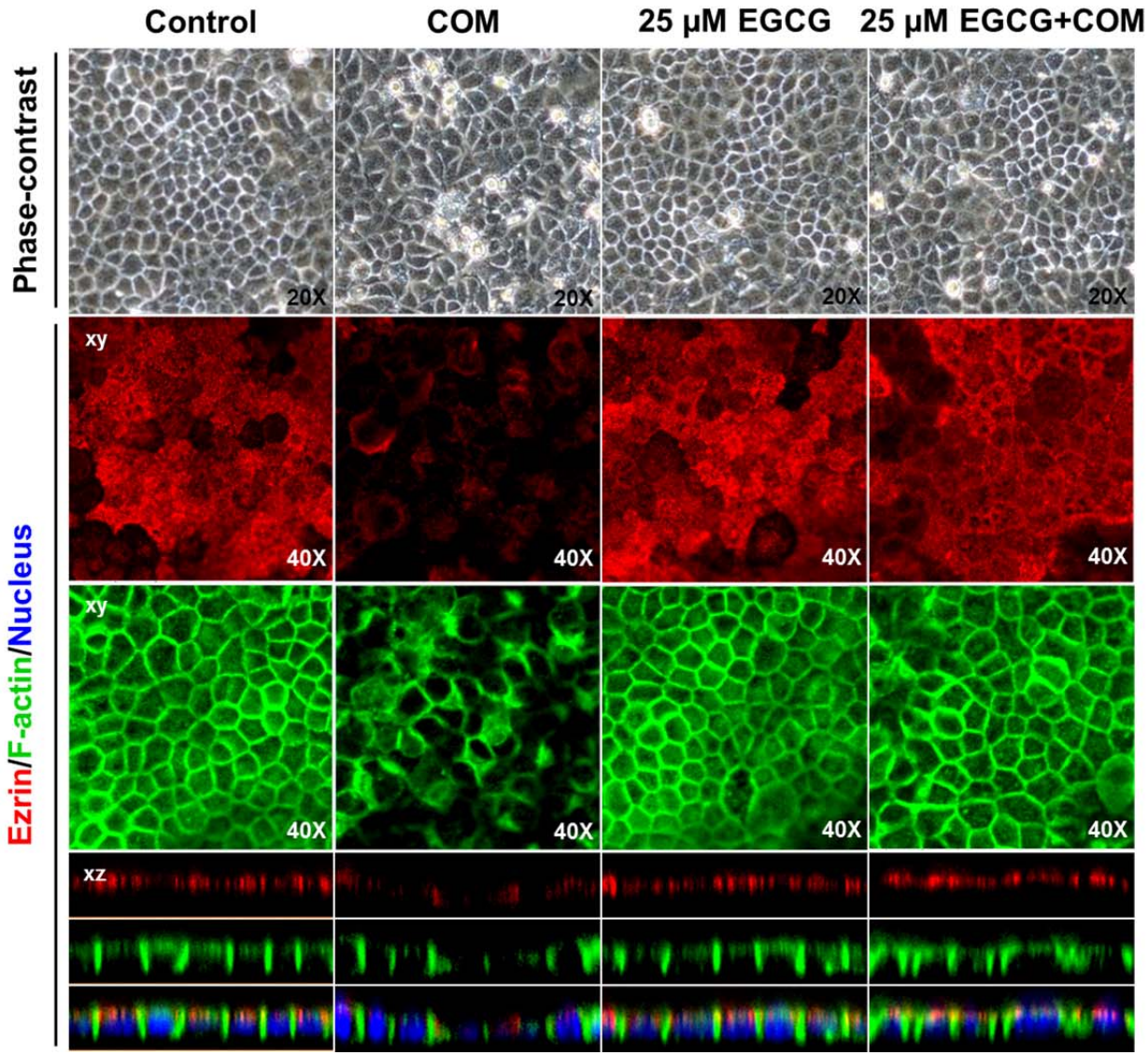
Control
COM
25 μM EGCG
25 μM EGCG+COM
Phase-contrast
20X
Ezrin/F-actin/Nucleus
xy
40X
xz

Figure 8

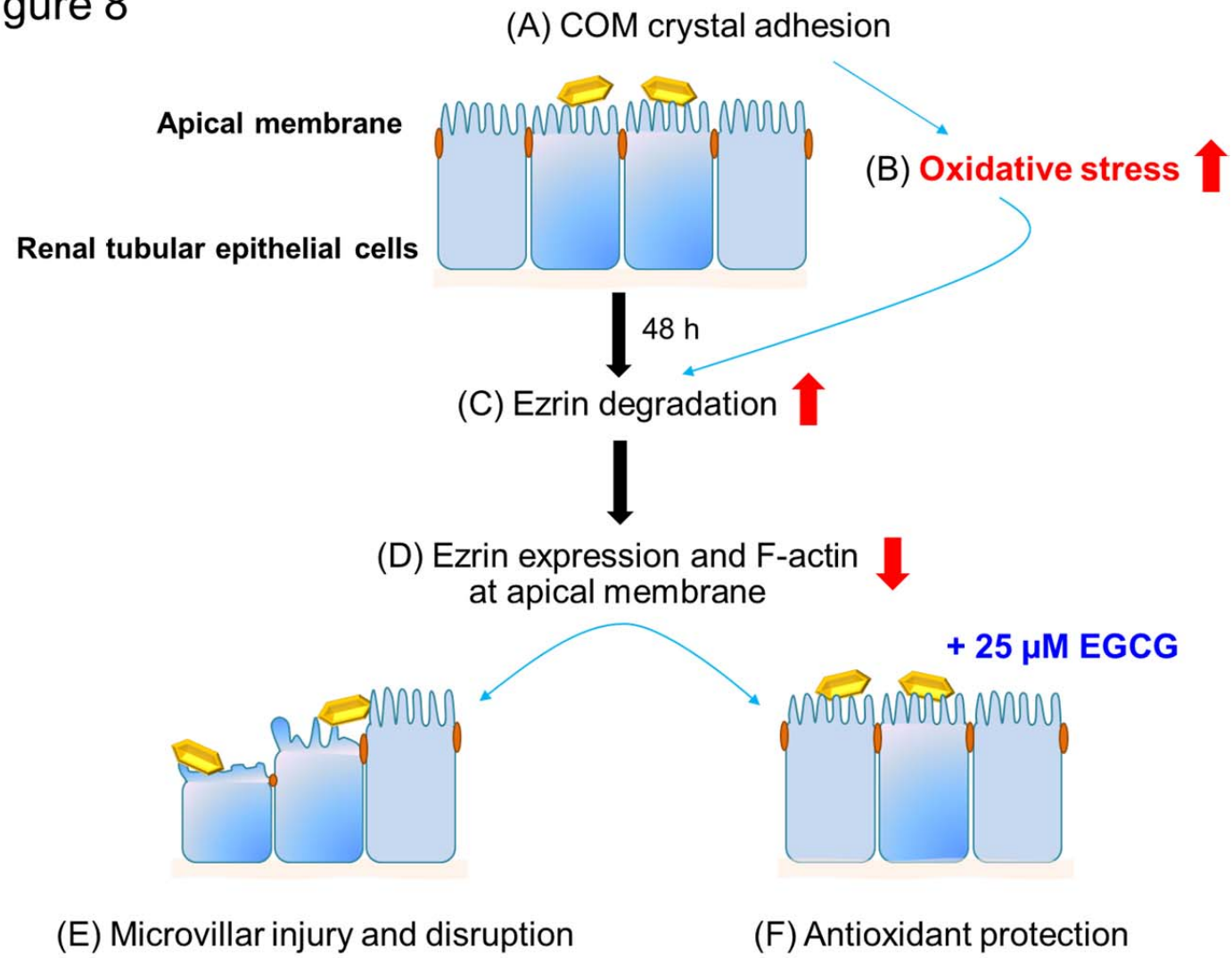
(A) COM crystal adhesion
Apical membrane
Renal tubular epithelial cells
(B) Oxidative stress
48 h
(C) Ezrin degradation
(D) Ezrin expression and F-actin at apical membrane
+ 25 μM EGCG
(E) Microvillar injury and disruption
(F) Antioxidant protection

Supplement 1

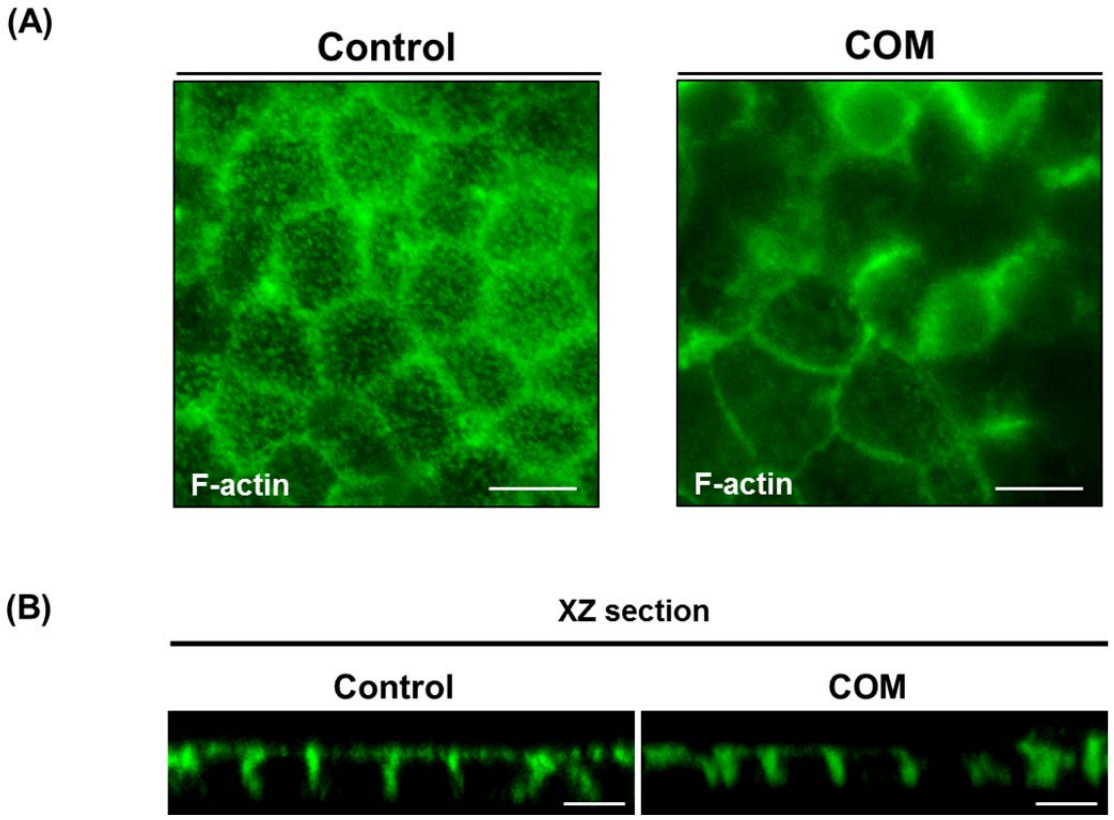

Supplement 2A

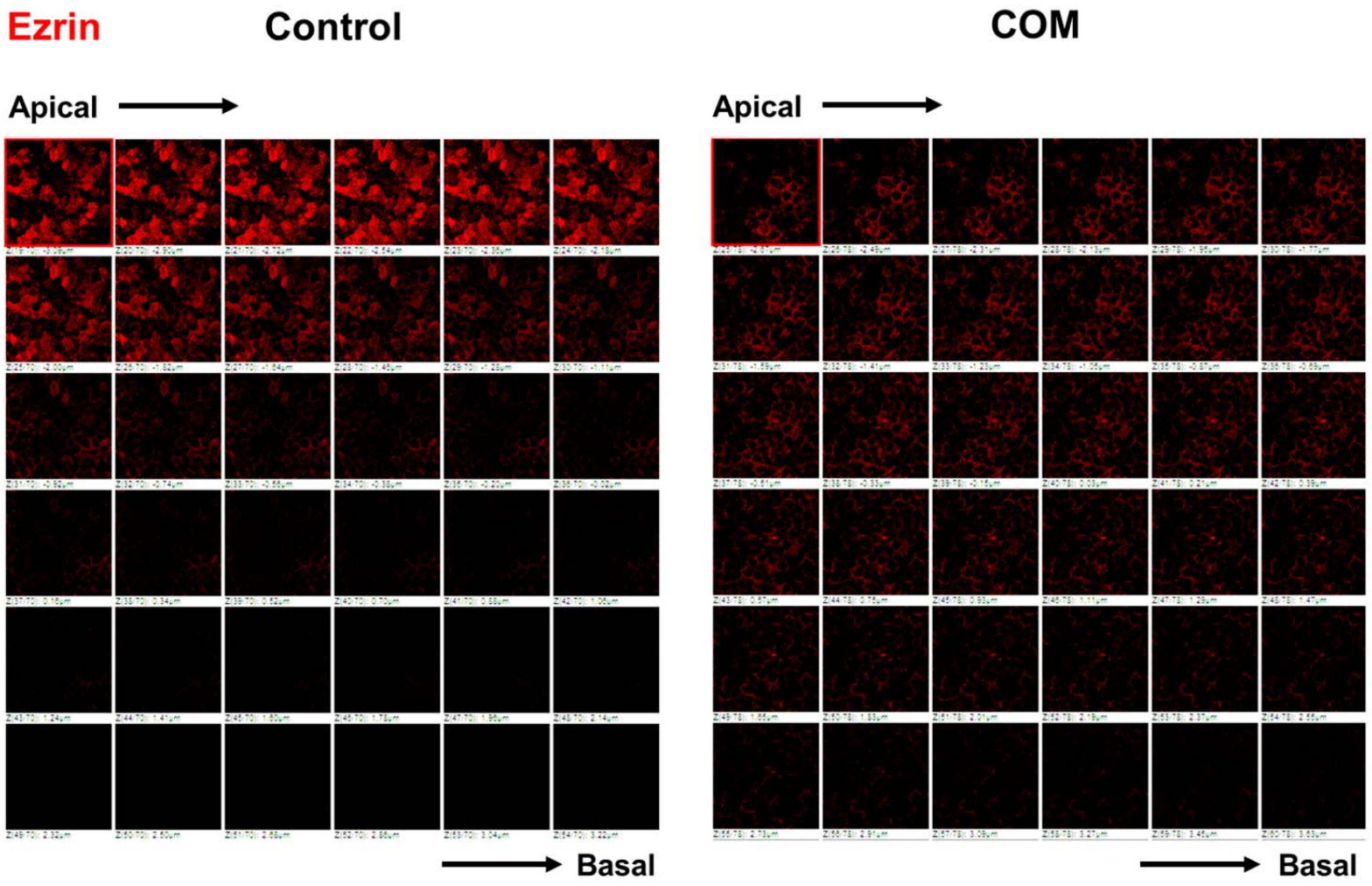

Supplement 2B

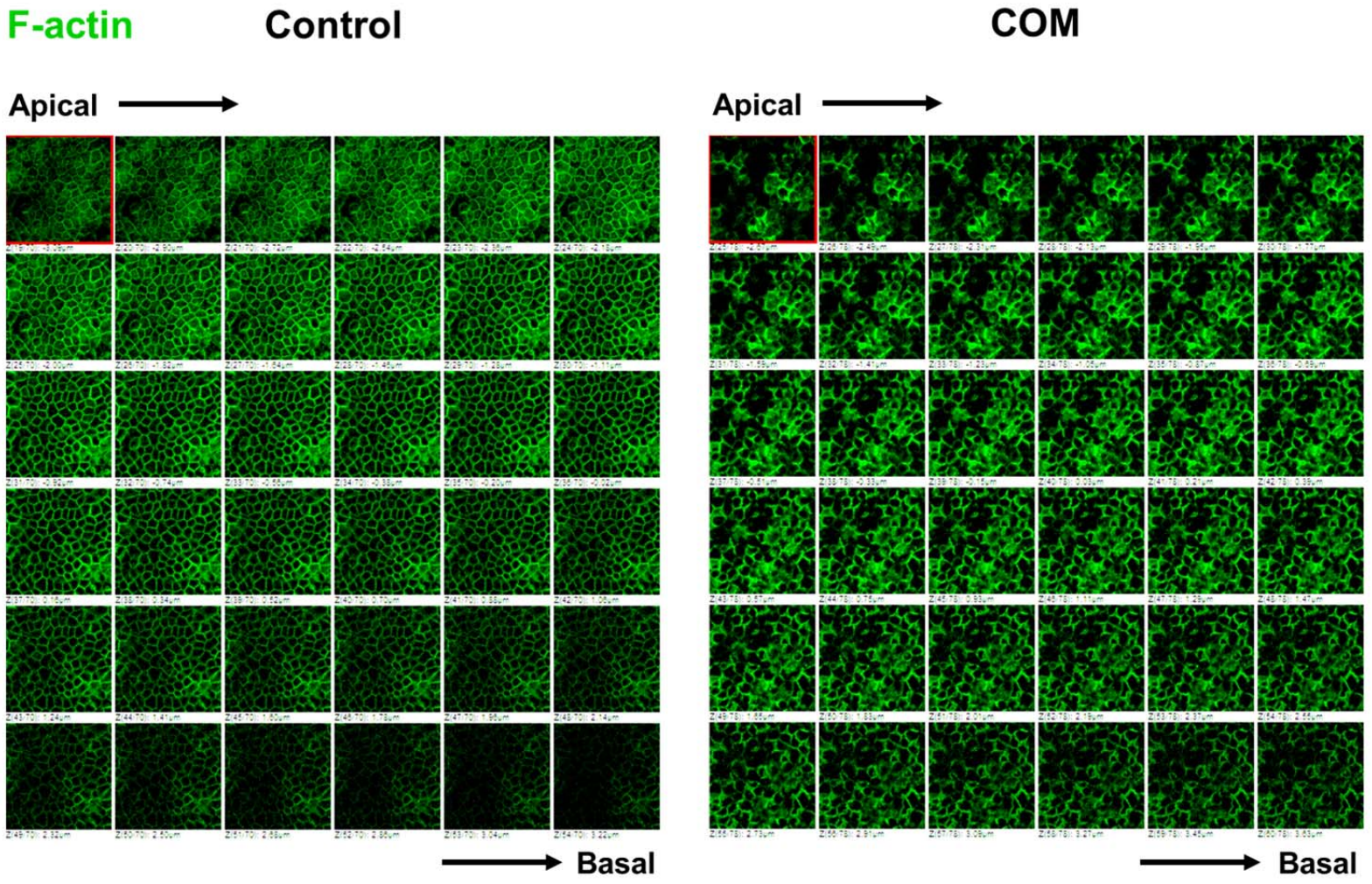

Supplement 2C

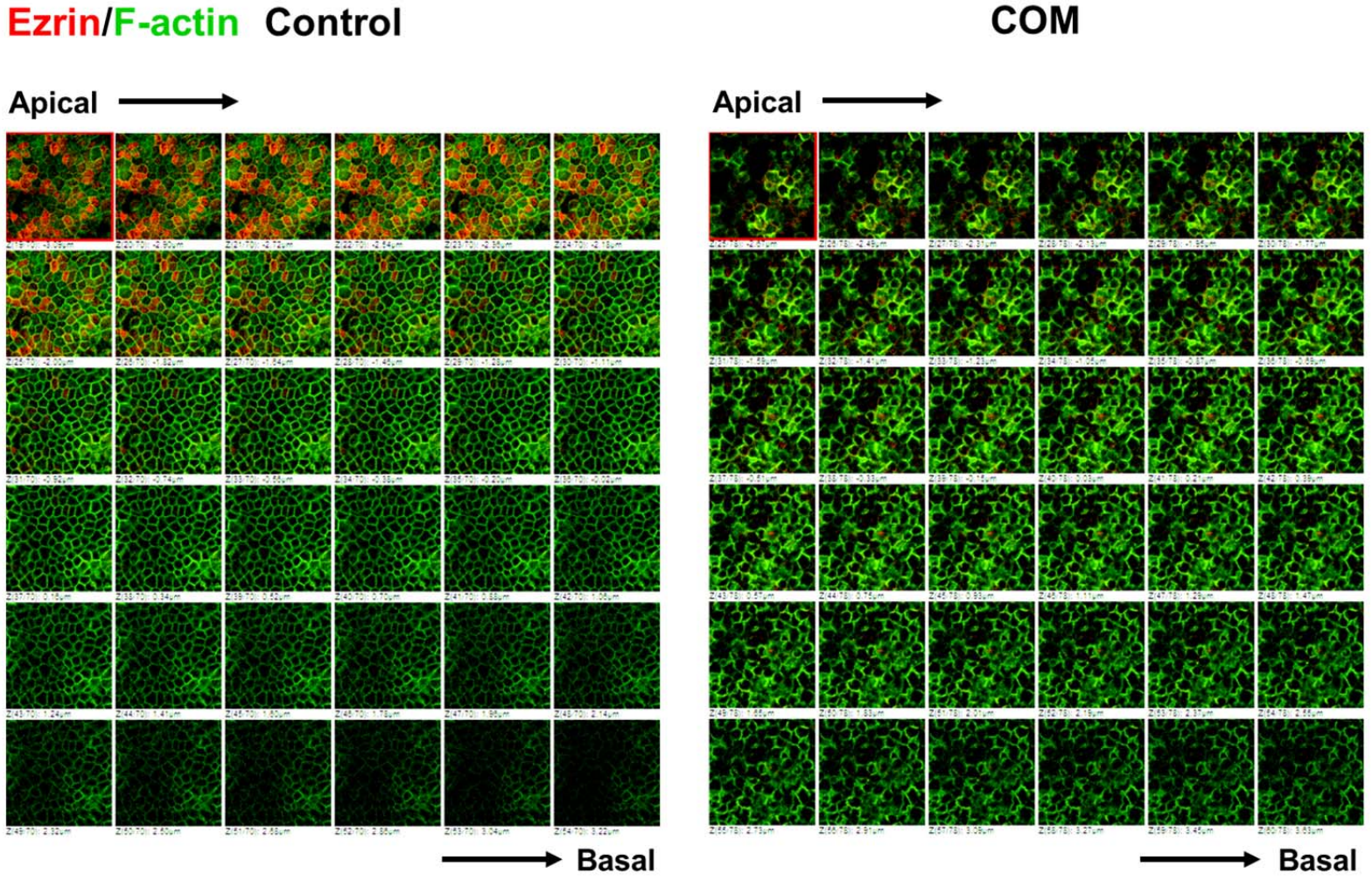

Supplement 2D

Nucleus **Control** **COM**